Simon-Philippe Breton

Study of the stall delay phenomenon and of wind turbine blade dynamics using numerical approaches and NREL's wind tunnel tests

Doctoral thesis for the degree of philosophiae doctor

Trondheim, June 2008

Norwegian University of Science and Technology
Faculty of Engineering Science and Technology
Department of Civil and Transport Engineering

NTNU

NTNU
Norwegian University of Science and Technology

Doctoral thesis for the degree of philosophiae doctor

Faculty of Engineering Science and Technology
Department of Civil and Transport Engineering

ISBN 978-82-471-1019-5 (printed version)
ISBN 978-82-471-1020-1 (electronic version)
ISSN 1503-8181

Doctoral theses at NTNU, 2008:171
Printed by NTNU-trykk

"N’est-ce pas dans le rêve cependant
que naissent la plupart des projets
qui en valent la peine?"

-René Lévesque

PREFACE

This thesis presents articles including the principal results following from the work accomplished during my PhD studies. I wrote these articles with the support from my supervisor Prof. Geir Moe. Other co-authors also contributed to this work, namely Prof. Frank Coton from the University of Glasgow, as well as Haiyan Long from the Norwegian University of Science and Technology. They are presented in the Results section of this thesis. The first article, entitled "*A Study on Different Stall Delay Models Using a Prescribed Wake Vortex Scheme and NREL Phase VI Experiment*", was published in the proceedings of the 2007 European Wind Energy Conference. The second article, "*A Study on Rotational Effects and Different Stall Delay Models Using a Prescribed Wake Vortex Scheme and NREL Phase VI Experiment Data*", was published in Wind Energy at the beginning of 2008. The third article, "*Assessment of Motions, Moments and Forces in the NREL NASA Ames Wind Tunnel Tests*", was submitted for publication in Wind Energy, while a slightly modified version of the fourth article presented here, "*Status, Plans and Technologies for Offshore Wind Turbines in Europe and North America*", was accepted for publication in Renewable Energy at the beginning of 2008.

TABLE OF CONTENTS

SUMMARY

The production of electricity from wind has experienced an enormous growth worldwide in the last 20 years. It is now widely seen as a serious alternative to more conventional energy production methods. Improvements are however still possible to make it more cost-effective. This can be done through a better understanding of the fundamental phenomena involved in the interaction of the wind with the wind turbine rotor. This growth in the production of energy from wind is expected to continue at a similar rate in the years to come, helped by the installation of wind turbines at sea, that is becoming a hot topic in the wind energy field today.

The phenomenon of stall delay affecting rotating wind turbine blades is an example of an aerodynamic phenomenon that is not yet fully understood. Several models exist to correct for this effect. Five such models were first tested within a vortex wake simulation code based on the modelling of a prescribed wake behind the rotor of the turbine. Comparison was made with wind tunnel test data acquired in head-on flow on a two-bladed 10.1 diameter wind turbine at the National Renewable Energy Laboratories (NREL) in 2000. It revealed a general overprediction of the stall delay effects, at the same time as great disparity was obtained between the different models. Conclusions from this work served as a starting point for a much more thorough investigation on this subject, where several models were tested in terms of different quantities using the same simulation code, and where the application of some of the models was improved. Overprediction of the loads was once again obtained when comparison was made to the NREL results in head-on flow, and none of the models was found to correctly represent the flow physics involved. The premises on which each of the models relies were discussed as a means of better understanding and modelling this

phenomenon. The important issue of tip loss was also covered, and guidelines were suggested to improve the modeling of the stall phenomenon which involves very complex aerodynamics.

The NREL wind tunnel results were further scrutinized in term of the root flapwise and edgewise bending moments. This allowed to study the dynamics of the NREL blades, at the same time as verifying the consistency between these moments and different loads measured in these tests. Measurements of these moments at the root of the rigid NREL blades in head-on flow showed vibrations corresponding to the two first oscillation modes of the blades, in respectively the flapwise and edgewise directions. These features observed in both an upwind and a downwind configuration were presumed to follow from the presence of the tower. In the downwind configuration, dynamic effects affecting one blade when going through the shadow of the tower were found to be transmitted to the other blade in both the teetered and the rigid configurations. Modelling of the root edgewise and flapwise bending moments was performed by calculating two dynamic estimates based on forces measured respectively along the blade and in the hub region. The simulations generally reproduced the dynamic effects well, and they suggested a systematic error in the measurement of the root flapwise bending moment in the upwind configuration. Inaccuracies in measuring the tangential forces on the blade at high wind speeds were also detected.

Offshore wind energy, that is expected to soon lead the development of the wind energy technology, was thereafter studied, where downwind turbines that were given special attention in the dynamic analysis above might reveal themselves as a more adapted solution. The many advantages as well as challenges related to this technology were acknowledged. The status of this technology was investigated in both Europe and North

America, and it revealed that Europe is in advance regarding all aspects of wind energy over North America, where it still is at a planning stage. Important plans were however found to exist in North America, where the conditions for the installation and operation of wind turbines offshore are different. Many new solutions that might be better adapted offshore were also discussed, along with the possibility to use floating wind turbines.

1. INTRODUCTION

Wind energy technology has evolved tremendously since the end of the nineteenth century, when around 100 000 windmills were disseminated throughout Europe[1] and used the energy contained in the wind to perform different tasks, as for example grinding grain and sawing wood. It has now become a widespread industry generating enormous amounts of clean electricity. At the end of 2007, 57 GW of wind energy were installed in Europe, and 94 GW worldwide[2].

The oil crisis in the 1970s gave a first significant start to the industry we know today, when the issue of energy security arose, at the same time as it was realized that energy supplies should be diversified. Following this crisis, many turbines were quickly installed in the 1980's in the U.S., mostly in California. The design of many of these turbines was however found to be poor, which led to the more cost-effective and reliable turbines designed in Europe, mainly in Denmark, to impose themselves in the market. Ultimately, after many designs were tried and abandoned for different reasons, the classic Danish turbine, a three-bladed, upwind, horizontal axis wind turbine became predominant in the wind energy market[1].

As space for installing onshore wind turbines has begun to be more scarce in Europe, offshore wind energy has recently appeared as an alternative. It is now expected to constitute the next big step in wind energy development, as well as to drive the research and development in this field in the years to come[1]. Since virtually no size limit exists for the installation of wind turbines offshore, the clear increasing trend on the size of wind turbines that has been observed since the 1980s[1] is expected to continue. Rotor blades of more than 60m are now being used, and as they grow longer, they also become more flexible, which leads to dynamic motions taking on more importance.

Wind turbine aerodynamic efficiency has progressively increased since the 1980s, and is now close to the theoretical limit dictated by the Betz limit[3]. Little is therefore to be gained on this side. Improvements are rather attainable towards performing more reliable predictions of aerodynamic loads that would lead to more optimal designs, thus avoiding the over-designing of components following from uncertainties in the predictions. This would result in a decrease of the overall costs of wind energy, as aerodynamic loading is seen as a principal determinant of these costs[4]. Reliable predictions of aerodynamic loads necessitates the use of accurate modeling methods. The accuracy of such methods is very dependent on a correct understanding of the complex flow mechanisms involved in wind turbine blade aerodynamics. Many such mechanisms are still far from being thoroughly understood, see for example Coton et al.[5], or the review articles by Hansen et al.[6], Leishman[7], and Snel[8]. They include among others stall delay, dynamic stall, as well as the effects from dynamic inflow, tower shadow, and structural dynamics of the blades. In order to study these mechanisms, and thereby, the accuracy of existing prediction models, the predictions have to be tested against reliable experimental data measured on realistic model wind turbines under controlled input conditions. A real need for such data that had been long present in the wind energy community[5,9] was addressed by wind tunnel tests performed in 2000 on a 10.1m diameter turbine in the biggest wind tunnel in the world located at the National Renewable Energy Laboratories (NREL) in the US.

Following the NREL wind tunnel tests, modeling experts in the wind energy field around the world were invited to participate in an anonymous exercise where they should use their modeling tools to predict loads and performance in a selected number of operating conditions, without having access to the experimental results. This was

referred to as the blind comparison exercise. A report was produced following this exercise, which compared the predictions with the measurements, and it pointed to surprising results[10]. One of the main conclusions from this report was that "*Blind comparisons were not favourable*". Significant differences were in fact observed between predictions and measurements, even in conditions expected to be easy to model, for example under steady inflow and at low wind speed, where stall is not an issue. Large discrepancies were generally also found at higher wind speeds. Fig. 1 shows an insert from this report, where comparison is made between the measured and predicted low-speed shaft torque and root flap bending moment. The predictions shown here were found from performance codes relying on the Blade Element Momentum method. Significant differences are observed between the predictions and measurements of these quantities. Features worth noting concern the general discrepancies seen at low wind speed in the case of the root flap bending moment, and at high wind speed for the low-speed shaft torque.

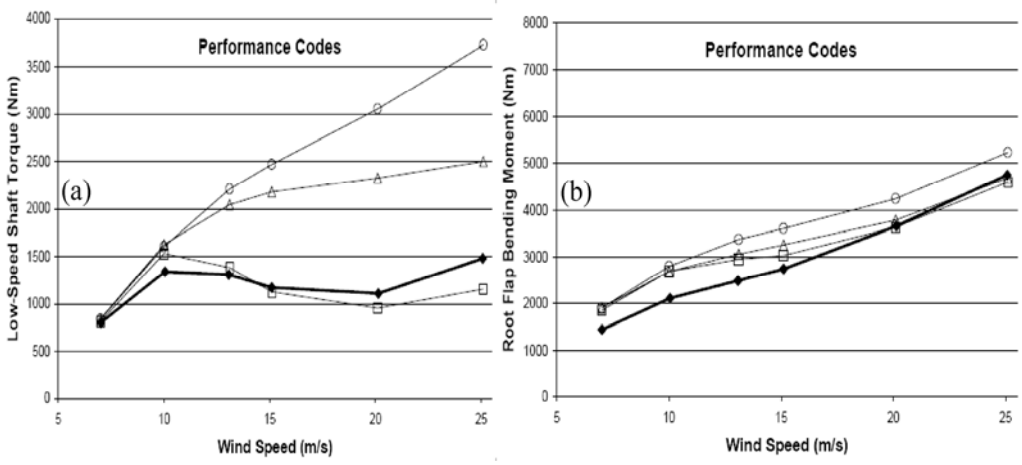

Figure 1. (a) Low-speed shaft torque and (b) Root flap bending moment: comparison between measurement (full diamonds) and predictions obtained from performance codes (empty symbols). (Adapted from Simms et al., 2001) [10]

These results concern integrated quantities. Problems were also obtained when predicting local loads on the blade. All of this raised a number of specific issues, leading to suggestions on phenomena requiring further study. Stall delay effects were for example hypothesized to be one of the main causes for the discrepancies observed at high wind speeds in the presence of stall. This was among other things observed through significant underpredictions of the normal force in the root region, and this suggested that better ways to model the stall delay phenomenon should be developed. Overprediction of loads in the tip region indicated that the tip loss issue necessitated further investigations. The significant discrepancies observed at low wind speed for the root flap bending moment raised important questions, and results obtained in the downwind configuration suggested further analysis concerning the effect of the tower shadow on the rotor of the turbine.

These issues raised by NREL's blind comparison report served as a starting point for the work accomplished here and presented in this thesis. It followed one of this report's conclusions stating that the problems addressed should be attacked by aggressive, targeted exploitation of the NREL wind tunnel test results[10]. The stall delay phenomenon having been found not to be correctly understood and modelled, a study on this subject was undertaken. Five existing models intended to correct two-dimensional airfoil data for rotational effects leading to the stall delay phenomenon were tested with the help of a prescribed wake vortex simulation code, and results were compared to the NREL wind tunnel test data. This led to the writing of the first article reproduced herein, presented at the European Wind Energy Conference in 2007. Conclusions from this work suggested to push the study further, as well as ways to do so. In the second article, published in Wind Energy, more models are tested, and the application of some

of them is improved relative to the first article. Moreover, the measured root flap bending moment is studied instead of the thrust. The former was measured at the root of the blade with strain gauges and is thus expected to be more reliable than the latter which was estimated from pressure measurements. Forces along the blade are also investigated instead of the corresponding non-dimensional coefficients, because they inform more about the actual loads acting on the blades. This article is much more extensive and goes far deeper in terms of analysis and understanding of the stall delay phenomenon. In addition to the stall delay issue, it treats the very important aerodynamic effects occurring in the region of the tip.

The study of the root flap bending moment that was made in the second article pointed towards significant differences between the measured and simulated root flap bending moment in terms of mean value. Similar discrepancies were also seen concerning a root flap bending moment calculated from forces measured along the blade. This, together with a conclusion from NREL's blind comparison report[10] regarding discrepancies at low wind speed in terms of root flap bending moment predictions, as well as access to two estimates for the root flap bending moment calculated by NREL in order to cross-check the measurements[11], suggested further work on this quantity. This was undertaken in a conference article[12] (not shown here) also presented at the European Wind Energy Conference in 2007. The root flap bending moment was there studied in the downwind teetered configuration as a function of azimuth angle, where interest was by the way raised concerning dynamic effects triggered by the passage of the blades through the shadow of the tower. These effects were clearly visible through the measured root flap bending moment, which showed the excitation of vibration modes. Measurements were compared with the two above-

mentioned estimates, based respectively on measured aerodynamic forces and on forces measured within the hub region. Both estimates were shown to significantly differ from the measurements. Although the calculation of the second estimate was improved in this conference article, discrepancies remained. Unresolved issues and conclusions from this article led to a much more extensive work on the subject, presented in the third article shown herein. In this journal article, submitted in Wind Energy, both the rigid and teetered configurations of the hub are investigated, for downwind as well as upwind operation. The calculation of the estimate based on forces measured within the hub region is modified relative to the above-mentioned conference article. The estimate based on the aerodynamic forces is also improved. Following recommendations from this conference article, a model to account for tip loss is included, as well as a new way of considering the measured force distribution along the blade. Dynamics is further included in its calculation with the help of a model based on the Finite Element Method built with the software Ansys. The downwind rigid configuration using a high cone angle (18 degrees), significant effects on the root flap bending moment result from the centrifugal force, which has to be carefully considered. The root edgewise bending moment is likewise investigated in this journal paper which presents a study of structural dynamics effects affecting the blades of a rotating wind turbine, investigates the effect on the rotor from the presence of the tower, and allows to verify the consistency between the forces and moments measured on the NREL turbine.

Downwind turbines that were given special attention in the third article presented here are of great interest for offshore applications, where they have many advantages over upwind turbines and could constitute one of the more optimal solutions adapted to offshore wind energy. This led to a study on offshore wind energy

technology, which took the form of a journal article that was accepted for publication in Renewable Energy, where focus was made on new technologies that could be developed specifically for offshore wind turbines.

Let us note that the experimental methods, results as well as discussion are included in the articles presented. However, before the articles is found a short section giving more information about the NREL wind tunnel experiments, which are at the center of the studies performed, as well as a section introducing basic notions about the phenomenon of stall, which is central to the two first articles presented below. A section entitled “Discussion and Conclusions” is also included following the articles in a synthesis perspective, and as a way of discussing in more details subjects that were treated quickly in the articles due to space limitations. This last section also allows to conclude on the work performed, as well as to suggest ideas concerning future research. Before going further, let us summarize the aims of the studies performed.

2. AIMS OF THE STUDY

The aims of the present study were to:

• Contribute to a better understanding of stall delay effects following from the rotation of wind turbine blades by analyzing and testing existing models intended to correct airfoil data for these effects, using a prescribed wake vortex scheme and NREL wind tunnel test data

• Analyze, better interpret and model structural dynamic effects affecting an operating wind turbine in both a downwind and an upwind configuration, with special attention given to the effects caused by the presence of the tower, through the use of NREL wind tunnel test data for the root bending moments as well as dynamic estimates calculated for these quantities. Use these estimates as a tool to verify the consistency between these moments and different loads measured in the NREL tests.

• Make an investigation of the status and plans for offshore wind energy development in Europe and North America, of the advantages and challenges linked to this technology, and of new possible solutions better adapted to offshore wind turbines.

3. EXPERIMENTAL DATA: NREL WIND TUNNEL TESTS

In this thesis, reference is often made to wind tunnel tests from the National Renewable Energy Laboratories. These tests were performed in the year 2000, in the biggest wind tunnel in the world (24.4 x 36.6 m), on a 10.1m diameter model wind turbine. Fig. 2 shows the wind turbine in question. It is a two-bladed stall-regulated turbine whose nacelle is supported by a 0.4 m diameter cylindrical tower at a hub height of 12.2 m. Tests were performed in many different configurations including upwind/downwind operation, teetered/rigid hub, flat/coned, yawed/non yawed, rotating/parked rotor, etc. In the rotating configuration, the rotational velocity was fixed at 71.6 rpm.

Figure 2. NREL wind turbine in the NASA Ames wind tunnel. (From Schreck, 2001)[13]

Fig. 3(a) represents the blade used on the NREL turbine that was equipped with taps allowing pressure and thereby aerodynamic force measurements at five radial locations (0.3R, 0.47R, 0.63R, 0.80R and 0.95R, with R the blade span). Fig. 3(b) presents the pressure tap distribution around the airfoil section at the five radial stations, showing a

larger concentration near the leading edge. It also shows that the S809 airfoil section was used along the blade. In addition to the full pressure tap distributions, 10 partial distributions containing two taps on the suction surface at the 4% and 36 % chordwise positions were distributed along the blade, as also shown in Fig. 3(a).

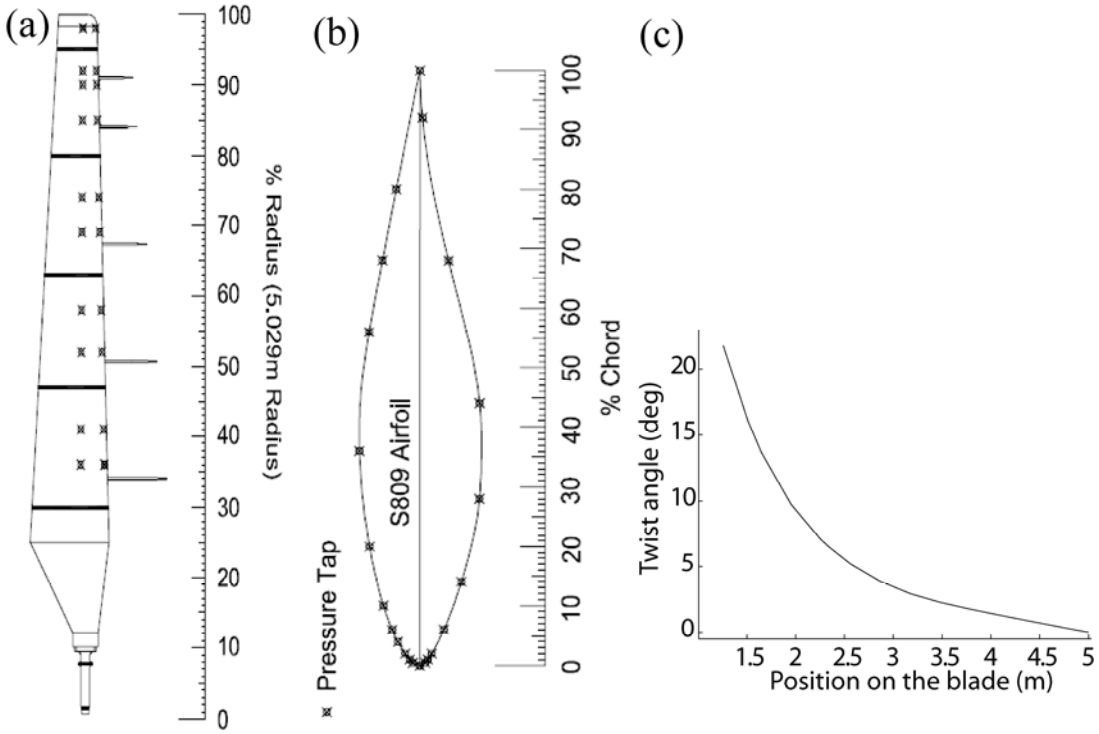

Figure 3. (a) Locations of the full (indicated by full lines) and partial (indicated by x) pressure tap distributions on the NREL blade, as well as of the 5-hole probes (indicated by lines ahead of the blade), (b) distribution of the pressure taps for the full distribution, (c) twist distribution along the blade. ((a) and (b) adapted from Hands et al., 2001)[11]

The blade was also equipped with 5-hole probes at five spanwise positions to measure the local flow angle ahead of the blade, at a distance corresponding to 80% of the chord (Fig. 3(a)). The other blade on the NREL turbine is geometrically identical to the blade shown, but includes neither pressure taps, nor 5-hole probes. One can note from Fig. 3(a) that the blades are tapered, the chord length diminishing from 0.737 m at the 25% spanwise position to 0.356m at the tip. The blades are also twisted, as seen in Fig. 3(c). Being both twisted and tapered, their geometry is representative of the blades used on

modern wind turbines. The NREL blades are however known to be more rigid than the latter. In addition to forces along the blade, forces within the hub region were measured, as well as the low speed shaft torque, and the root flapwise and edgewise bending moments.

These tests being performed in a wind tunnel, inflow conditions were rigorously controlled. This is the first time that such a large turbine was tested under strictly controlled input conditions. Tests have been performed in field conditions relatively recently on five turbines in a joint effort from different research institutes in studying the complex aerodynamic behavior of a wind turbine, referred to as IEA Annex XIV[14]. Diameters ranged from 10 m to 27.5 m, and pressure along the blades was also measured. This included tests on a wind turbine from NREL similar to the one described above. However, disadvantages related to field conditions where the wind environment is not controllable, leading for example to turbulence and variable wind direction, made it impossible to capture the reproducibility, accuracy and reliability that the NREL wind tunnel tests allowed[11]. These tests mark the first time in wind energy history that so large amounts of data of such accuracy were obtained. They therefore provide the wind energy community with a unique and long awaited for opportunity to study many different aspects of aerodynamics and structural dynamics of wind turbines.

4. THEORETICAL ASPECTS CONCERNING THE STALL PHENOMENON

4.1. Reynolds number

The notion of Reynolds number is central to the study of the interaction of fluids with bodies. This dimensionless number denoted as Re is defined as

$$\mathrm{Re} = \frac{\rho V d}{\mu} \text{ , where} \quad (1)$$

ρ=fluid density [kg/m^3]

μ=fluid viscosity [kg/(ms)]

V= free stream fluid velocity [m/s]

d=characteristic length dimension of the body [m]

4.2. Boundary layer

To describe the phenomenon of stall, basic notions concerning the boundary layer concept are necessary. This concept is the heart of a widely used approach denoted as boundary layer theory. This approach consists in computing the effects of viscosity, and thereby friction, inside a thin region close to the surface of a body, called the boundary layer, and to combine these with the behavior of the flow in an outer inviscid region where such effects are negligible. This outer region can then be described using potential theory[15]. As we will see, the phenomenon of stall is intimately linked to the separation of the boundary layer from the surface, which can be predicted by boundary layer theory.

The existence of the boundary layer comes from the fact that a moving fluid interacts with the surface, adheres to it, and therefore cannot move relative to it immediately at the surface. This is referred to as the no-slip condition. This results in a velocity distribution normal to the surface, starting with a zero velocity directly at the

surface, and increasing rapidly with normal distance, see Fig. 4, until it reaches free stream velocity. The thickness of the boundary layer is defined as the distance from the surface δ where the velocity reaches 99% of the free stream velocity. This thickness increases as the flow moves along the surface. The boundary layer is usually thinner the lower the viscosity, because the interaction with the surface is then smaller. Let us note that boundary layer theory is not valid for too small values of the Reynolds number, or high viscosity, because the boundary layer would then become too thick, departing from the thin layer approximation.

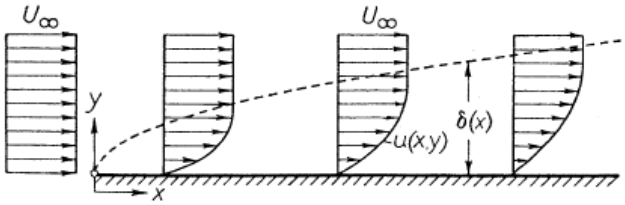

Figure 4. Velocity distribution in a boundary layer of thickness δ close to the surface of a body. U_∞=free stream velocity, u=local velocity. (From Schlichting and Gersten, 2000)[16]

The wall shear stress τ resulting from the interaction of the fluid with the surface is given by[16]

$$\tau_w = \mu\left(\frac{\partial u}{\partial y}\right)_w \tag{2}$$

where μ is the viscosity and $(\partial u/\partial y)$ is the velocity gradient normal to the surface (Fig. 4). The index w refers to the value directly at the wall, or surface. The velocity gradient normal to the surface is usually very large because the velocity has to increase from zero directly at the surface to 99% of the free stream velocity at the edge of the boundary layer quite rapidly, the boundary layer being thin. Consequently, even a small viscosity can result in a significant shear stress. Outside the boundary layer, the effect from the surface is no longer important, which results in small velocity gradients, and therefore negligible viscosity effects.

A drag force, referred to as friction drag, results from the viscous effects within the boundary layer. It is found from integrating the wall shear stress along the surface[15]. The total drag is found by adding the friction drag to the pressure drag, or form drag, which is the component of the drag resulting from the pressure distribution.

4.2.1. Types of Boundary layer and transition

The boundary layer for flow past a body can be of two types, namely laminar or turbulent. The nature of the boundary layer is dependent on the Reynolds number. For a Reynolds number below a certain critical value Re_{crit}, the boundary layer is laminar, while it is turbulent above this value. For example, for a smooth, flat plate at zero incidence, Re_{crit} has a value of 5×10^5.[16] An airfoil or blunt body would have a different critical Reynolds number. The laminar boundary layer is characterized by layers of flow moving with different velocities, where exchange of particles normal to the flow direction is almost non-existent. The situation is different for the turbulent boundary layer, which rather shows fluctuating motions leading to an important mixing normal to the flow direction.

For small distances travelled by the flow on the surface, the boundary layer will be laminar. However, after a certain distance, the laminar boundary layer will become unstable, and transition from a laminar to a turbulent boundary layer will take place.

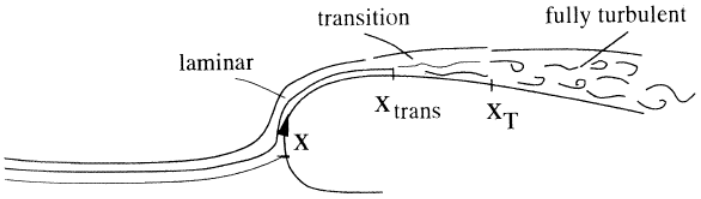

Figure 5. Boundary layer transition. (From Hansen, 2000)[17].

Fig. 5 illustrates this phenomenon on the surface of an airfoil. The location of the transition x_{trans} can be found by defining a local Reynolds number of the flow along the surface Re_x, with x the position on the surface[15] (Fig. 5):

$$\mathrm{Re}_x = \frac{Vx\rho}{\mu} \tag{3}$$

By equating this local Reynolds number with the critical value Re_{crit} defined above, the value x_{trans} at which transition occurs on that surface can be determined. This transition is characterized by an increase in the thickness of the boundary layer, as well as in the wall shear stress[16].

4.3. Separation of the boundary layer and stall phenomenon

The concepts of boundary layer separation and stall are intimately linked together. Stall is actually the consequence of boundary layer separation. Let us look more closely at these concepts, by first considering the role of the pressure distribution within the boundary layer.

4.3.1. Pressure distribution in the BL

Knowledge about the pressure distribution within the boundary layer is fundamental to predict its behavior on a given surface. Let us consider flow incoming on a body of a given geometry, for example an airfoil, at zero incidence. The shape of the airfoil will force the streamlines in the outer inviscid flow to curve around its geometry, giving rise to a pressure distribution on the outer edge of the boundary layer. This pressure distribution will be imposed onto the boundary layer, meaning that at every location along the airfoil, the pressure in the boundary layer normal to the wall is constant[16]. The pressure distribution directly at the surface will then be the same as the one at the outer edge, and is only a function of the position along the surface[16]. This

pressure distribution will dictate the displacement of the flow inside the boundary layer and is therefore a key quantity to predict the separation of the boundary layer from the surface. Two types of pressure gradients have very different implications for the flow moving along a surface. A favourable pressure gradient ($dp/dx<0$) has a suction effect on the flow which is naturally driven towards regions of lower pressure. An adverse pressure gradient ($dp/dx>0$) has the opposite effect, and is central to the obtention of separation. Usually, when a body is immersed in a flow, favourable pressure gradients are present on the front of the body, while adverse pressure gradients are found in the rear[15]. Let us now look more closely at how separation of the boundary layer happens in the case of a blunt body and an airfoil.

4.3.2 Examples of separation: blunt body and airfoil

Fig. 6 shows flow past a blunt body, in this case a two-dimensional cylinder. Fig. 6(a) shows the situation for real flow, while Fig. 6(b) illustrates inviscid flow. Fig. 6(a) also depicts the pressure distribution in the outer flow, that is imposed onto the boundary layer, as explained above. An interesting particularity about the cylinder is that it is symmetric, and therefore it has a symmetric pressure distribution. This will help explain the origin of the separation of the boundary layer.

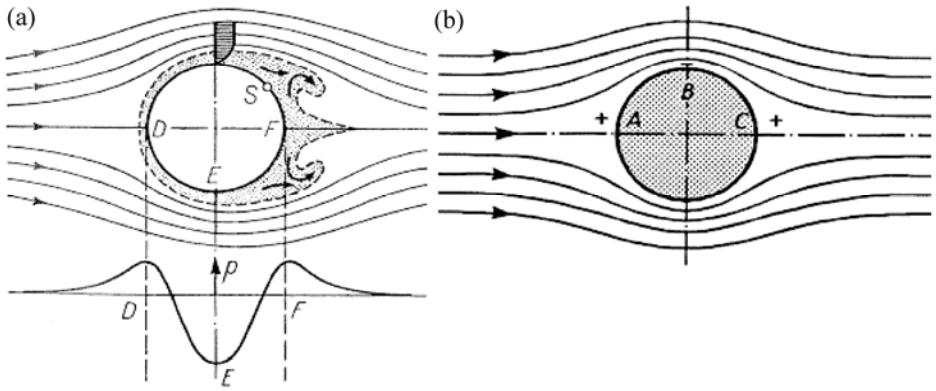

Figure 6. (a) Actual and (b) inviscid flow about a circular cylinder. (Adapted from Schlichting and Gersten, 2000)[16].

A constant interchange between the effect from the pressure gradient and kinetic energy is taking place. In the outer flow, when the pressure gradient is favourable, the flow particles accelerate, and pressure is transformed into kinetic energy. When the pressure gradient is adverse, kinetic energy is transformed back into pressure. However, in the boundary layer, friction forces come into play, and completely change the picture. In the case considered, the flow particle is accelerated from D to E (Fig. 6(a)) following a decrease in pressure (favourable pressure gradient), after which it is decelerated from E to F because of a pressure increase (adverse pressure gradient). If friction forces were not present, i.e., if the flow were inviscid, the situation would be symmetric, and the particles would manage to travel along the surface and reach the other side of the cylinder. We would then get smooth streamlines following the surface of the cylinder, as in (Fig. 6(b)). In reality, however, the flow particles within the boundary layer lose kinetic energy to friction all along the surface of the cylinder, making the situation not symmetric anymore. This implies that they no longer have enough energy to get over the pressure increase from E to F. The particles will stop moving, and then participate in a backflow because of the pressure distribution in the outer flow pulling them back towards the lower pressure at E. This corresponds to the separation of the boundary layer from the surface of the cylinder, as seen in Fig. 6(a) around point S.

The situation is different for an airfoil. Fig. 7 shows the pressure distribution on a symmetric airfoil at zero incidence. The pressure distribution imposed from the outer flow on the body is totally different from the case of the cylinder, and is not symmetric anymore. A strong favourable pressure gradient is first seen, going from A to B. This is

often referred to as the suction peak on the nose of the airfoil. This peak is followed by an adverse pressure gradient that is so small that the boundary layer will not separate[16].

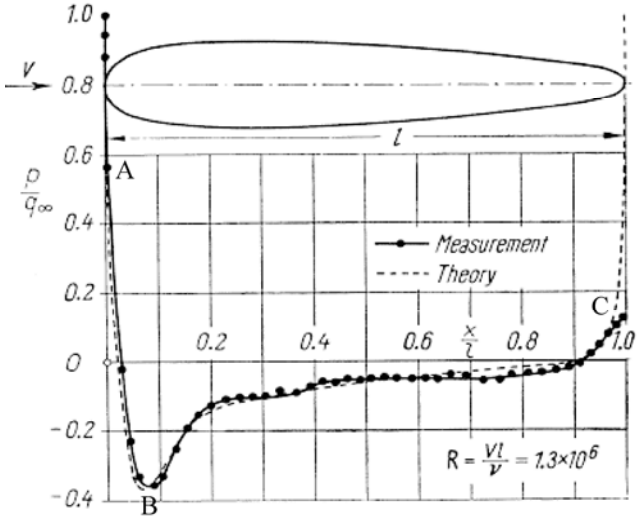

Figure 7. Pressure distribution on a symmetric airfoil. (Adapted from Schlichting, 1979)[18].

Such a small pressure gradient is obtained because the curvature of the wall further away from the leading edge is small[17]. Particles flowing along the surface in the boundary layer will be able to go from point A to point C without problem, even if friction forces slow them down along the way. The flow pattern is then smooth on the airfoil, which is qualified as a streamlined body. Backflow will therefore not occur, and neither will separation.

We get a different situation if we introduce an angle of attack, i.e. an angle between the incoming flow and chordline of the airfoil, see e.g. Corten[19]. In this case, the symmetric airfoil of Fig. 7 will experience a lift force. This lift force is associated with the presence of circulation around the airfoil in the form of a sheet of bound vortices[20]. These vortices indeed induce velocities on both sides of the airfoil. The velocity on one side of the airfoil finds itself increased by this additional velocity, while it is decreased on the other side. Following Bernoulli's equation, this creates a pressure

jump resulting in a lift force on the airfoil. An infinity of mathematical solutions are possible for this circulation found from integrating the bound vortices along the chord of the airfoil. The physical solution is determined by the Kutta condition[21] which states that the flow has to leave the trailing edge smoothly. With increasing angle of attack, the circulation around the airfoil as well as the lift produced will first increase, as known from airfoil theory[22]. The suction peak near the leading edge of the airfoil will then become stronger. Following Bernoulli's equation, the velocity in the outer flow near the suction peak will become very high. The suction peak is located near the stagnation point close to the nose of the airfoil, where the boundary layer is still very thin. A very thin boundary layer will imply that the velocity change normal to the surface of the airfoil will have to be very rapid for the velocity to go from zero at the surface (no-slip condition) to a very high value at the outer edge. As the wall shear stress is proportional to the velocity gradient normal to the surface directly at the wall (Eq. 2), very high friction forces will affect the flow and slow it down, adding to the effect of the adverse pressure gradient that follows the favourable pressure gradient related to the suction peak. The flow may not be able to reach the trailing edge anymore. It might get to a standstill, and go back towards low pressure values, leading to backflow and to the separation of the boundary layer from the surface. At this point, the airfoil is said to be stalled[15]. One can notice here the link between the separation of the boundary layer and the occurrence of stall. Let us now look at how the separation of the boundary layer can be predicted.

4.3.3 Prediction of the separation process

We saw above two qualitative examples that helped understand how separation of the boundary layer from a surface is possible. We will now describe how this

phenomenon can be predicted. Let us for this purpose look at Fig. 8, which shows the flow in the boundary layer over a given surface around a point S defined as the separation point.

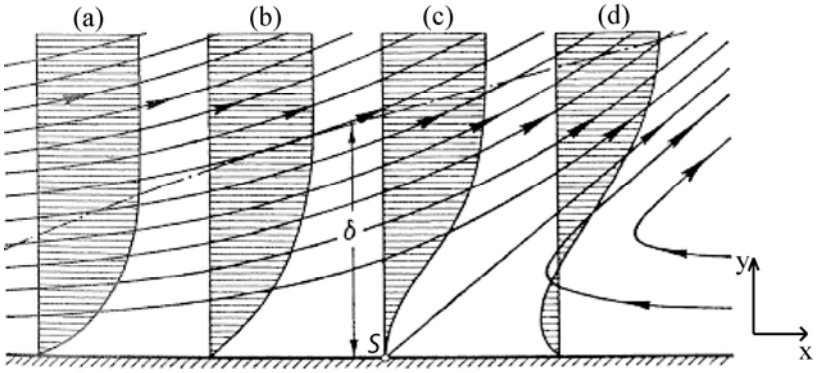

Figure 8. Boundary-layer flow close to the separation point S. (Adapted from Schlichting and Gersten, 2000)[16].

Before point S, the velocity gradient normal to the wall is seen to be positive, while it is negative after point S. Directly at S, it is equal to zero, which is the condition that determines the location of the separation point[16]:

$$\tau_w = \mu\left(\frac{\partial u}{\partial y}\right)_w = 0 \tag{4}$$

i.e., at the separation point, the friction shear stress defined above vanishes. It can be seen how this condition is linked to the presence of backflow mentioned above. When the flow has passed the separation point, the negative velocity gradient normal to the surface means that the flow velocity decreases when moving away from the surface, which results in backflow. The separation point then finds itself at the limit between positions of forward and reversed flows.

Hansen[17] explains further, using a geometric argument, the relation between the velocity profiles above (Fig. 8), the pressure gradients, and the occurrence of separation.

From the Navier-Stokes equation in the x direction applied directly at the wall, where the velocity is zero, we obtain

$$\left(\frac{\partial^2 u}{\partial y^2}\right)_w = \frac{1}{\mu}\left(\frac{\partial p}{\partial x}\right)_w \tag{5}$$

This indicates that the curvature of the velocity profiles at the wall is directly linked to the sign of the pressure gradient. We know from the definition of the boundary layer that the velocity gradient normal to the surface is equal to zero at the outer edge of the boundary layer. The curvature of the velocity profile for a negative pressure gradient will therefore be negative in the whole boundary layer, as in cases (a) and (b) in Fig. 8, meaning that a point of inflexion is not present. This curve shape corresponds to a situation where the boundary layer will not separate from the surface, i.e. where a favourable pressure gradient is acting on the flow. However, for a positive pressure gradient, the curvature of the velocity profile will be positive at the wall, necessitating a point of inflexion somewhere in the velocity profile. This corresponds to an S-shaped curve, seen for example in cases (c) and (d), and that could also be represented by intermediary situations between (b) and (c)[17]. An S-shaped curve being related to an adverse pressure gradient, separation may occur in this case.

4.3.4. Consequences of separation

The separation of the boundary layer, and thereby, the occurrence of stall, is accompanied by a significant thickening of the boundary layer, explained among other things by the occurrence of reverse flow discussed above. This leads to the formation of a large region of "dead water", where the fluid is not moving and the pressure is the same as in the free stream[23]. Vortices are also formed from the backflow in the detached boundary layer. They will eventually separate from the body into a low pressure wake,

mix with the outer flow, and be transported with it. This interaction between the separated boundary layer and outer flow, seen among other things by a deflection of the mainstream, will make the outer flow and its pressure distribution different from the prediction from inviscid theory that could be used in the boundary layer theory analysis when added to the effect of the boundary layer close to the surface. This makes boundary layer theory invalid after separation. For a lifting body, this also creates a rupture of the inviscid lift-producing flow[16], resulting in a loss of lift, which is one of the most important consequences of stall. This is seen in lift polars (see e.g. Abbott and von Doenhoff[22]), where from a certain angle of attack the lift does not continue to increase with the angle of attack, but rather begins to go down. The start of the separation of the boundary layer from the airfoil surface is actually known to approximately coincide with the maximum lift of the airfoil[16]. A large increase in the pressure drag is also resulting from the separation of the boundary layer. This is explained by the strong negative pressure in the region that is filled with the vortices from the backflow[16], or more specifically by the difference between the high pressure in the region near the stagnation point, and the low pressure in the rear region of separated flow[15].

Avoiding separation is therefore an effective way of limiting the occurrence of drag, as before separation, the total drag is mostly consisting in friction drag which is usually small. This can be achieved by streamlining a body, which helps prevent separation, as discussed above. Let us quickly look at other ways that can help avoid separation.

4.3.5 Ways to prevent separation

Schlichting and Gersten[16] suggest different methods to avoid separation of the boundary layer from a surface, or delay its occurrence. Using a slit, suction can be used to suck the flow towards the trailing edge of an airfoil, helping it overcome the friction forces and adverse pressure gradient, avoiding separation and allowing an increase in the maximum lift. In a similar way, blowing air through a slit in the direction of the flow could provide it kinetic energy, helping it to travel along the surface and reach the trailing edge, therefore preventing separation. It is also possible to influence the pressure distribution on an airfoil by positioning a slat on its surface, which helps avoid positive pressure gradients and thus separation.

Let us note, however, that stall does not only have negative consequences, and efforts are not always made to avoid it. Stall can indeed be made use of as a tool to limit the power produced by wind turbines at high wind speed, an approach referred to as stall control. It constitutes one of the methods used today on modern wind turbines to insure that they do not exceed nominal power. The other method is pitch control, where the blades are rather pitched to decrease the angle of attack and therefore the aerodynamic forces to which they are subjected.

Let us now look at important implications that the rotation of the blades has on the occurrence of stall.

4.4. Stall delay

We presented above active ways that could be used to prevent stall or delay its occurrence. Rotation was also found to have a delaying effect on the occurrence of separation, as first observed by Himmelskamp on aircraft propeller blades[24]. Although they do not constitute an active way to prevent stall as the methods mentioned above,

rotational effects are at the origin of a phenomenon which is referred to as rotational augmentation, or more commonly, as stall delay. This phenomenon will now be introduced shortly.

4.4.1. Observation in experimental results

The delaying effect that rotation has on the occurrence of stall is illustrated in Fig. 9, taken from the work of Ronsten[25], who performed pressure measurements on a rotating and a non-rotating blade.

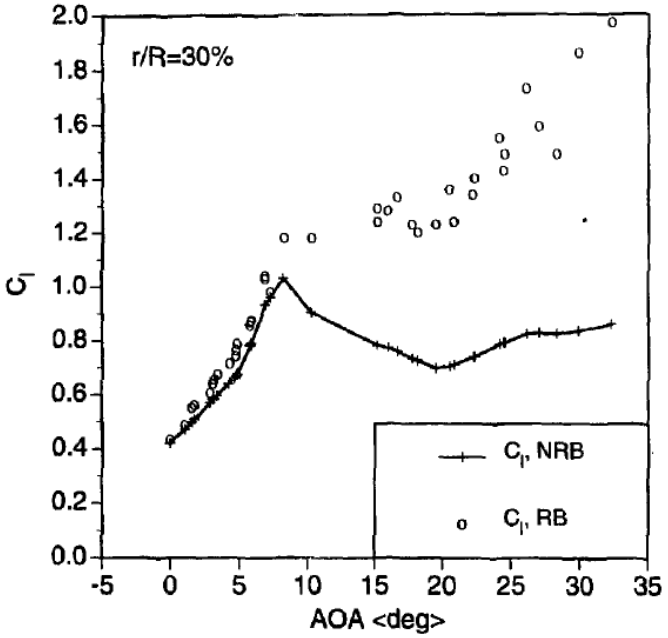

Figure 9. Lift coefficient C_l measured at the 30% spanwise position on a rotating (RB) and non-rotating (NRB) blade as a function of angle of attack. (From Ronsten, 1992)[25]

This figure compares the lift coefficient measured in these two conditions at the 30% spanwise position, plotted as a function of the angle of attack. It is clearly seen that the occurrence of stall is delayed by the rotation, and that a higher maximum lift is reached when the blade is rotating.

After having first been noticed on aircraft propeller blades as mentioned above[24], stall delay was also observed and studied on helicopter blades (see e.g. Dwyer and

McCroskey, 1971)[26], and later on wind turbine blades (see e.g. Milborrow, 1985)[27]. This delaying effect from rotation has been found to be more present in the region closer to the root of the blade, where higher angles of attack are reached due to a lower rotational velocity. It is also clearly present in the wind tunnel test data measured on the NREL stall-controlled wind turbine[11], as will be discussed in the two first articles presented below.

We will now briefly introduce the most important factors following from rotation that may play a role in the delay of stall, before a more thorough investigation of this phenomenon and of existing methods to model it is performed in the two first articles below.

4.4.2. Main effects responsible for stall delay

It has been observed experimentally that separated flow on a rotating blade has a strong component of radial velocity, see for example McCroskey[28]. CFD simulations have also shown similar features, as observed in Fig. 10, which presents calculated streamlines on the NREL rotating turbine blade at an incoming wind speed of 10m/s. It is seen in this figure that separated flow, which is more present in the root region, has a much larger spanwise motion than attached flow, which rather travels smoothly in a direction almost parallel to the chord of the blade. This feature helps understand mechanisms involved in the stall delay process. It is one of the main differences from the non rotating case, and one can await that it plays a significant role in the stall delay process. We will come back shortly to this spanwise flow, and to its causes and consequences.

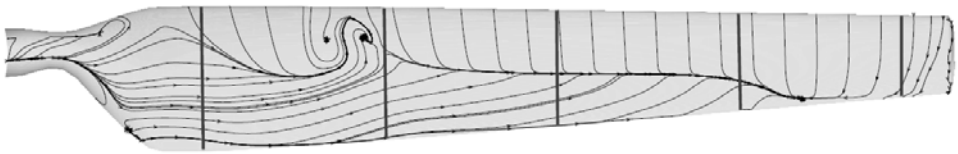

Figure 10. Limiting streamlines on the suction side of the NREL rotating blade for an incoming wind speed of 10 m/s. (From Sørensen et al.)[29]

Rotation has two main effects on the behavior of the flow. First, it causes the dynamic pressure along the blade to increase towards the tip, because the relative wind velocity seen by the rotating blade increases with radial position. Second, it leads to the appearance of two external forces when one places itself in a rotating frame of reference, namely the centrifugal and Coriolis forces. These effects will act differently on attached and separated flow.

The varying dynamic pressure along the blade and the centrifugal force are expected to give a radial velocity component to the attached flow. The effect of the former is explained by the proportionality of the chordwise pressure distribution to the dynamic pressure[30], creating a spanwise pressure gradient that directs the flow towards lower pressure and therefore higher radial positions. When the boundary layer is attached on the rotating blade, the flow does not stay long on the blade and therefore does not have much time to move in the radial direction on the blade[19]. However, the fact that it has a radial velocity component results in the appearance of a Coriolis force, directed towards the trailing edge. This Coriolis force acts as a positive pressure gradient and therefore delays separation. It has a similar effect as that obtained from blowing air in the chordwise direction of an airfoil, which was mentioned above as an approach to prevent boundary layer separation.

Rotation has a different effect on the separated flow itself. As mentioned above, separation is observed when the air in the boundary layer comes to a standstill in the

chordwise direction due to the effects from the friction forces and adverse pressure gradient. The separation point was further defined as the position where the gradient of the chordwise velocity taken in a direction normal to the surface zeros out at the surface (see Fig. 8 and Eq. 4). This is the same in the rotating situation, when the effect from rotation is intrinsically included in finding the separation position from the conditions mentioned above. This means that a "dead-water" region will also be formed in this case. In order to have such a region of flow at standstill, an equilibrium of chordwise forces will have to take place. These forces are the Coriolis force and the effect from the chordwise pressure gradient[19]. The fact that the separated flow does not move chordwise relative to the blade implies that the centrifugal force is now pushing at every instant radially outwards on the separated flow, while in the attached flow case it could only act for a short time on any material volume. The centrifugal force is then said to have a pumping effect on the separated flow[30]. The existence of the Coriolis force in this case results from the radial motion of the separated flow. A close interaction is then seen to exist between the Coriolis and centrifugal forces. The existence of radial flow in this case is supposed by Lindenburg[30] to come mostly from the centrifugal force and not from the spanwise pressure gradient. He explains it by saying that the separated area of flow close to the trailing edge has a pressure which is close to the atmospheric pressure. This suggests in this case that the chordwise pressure distribution only has a small spanwise gradient, which would lead to a negligible contribution to the radial flow compared to the effect from the centrifugal force. The radial motion of the separated flow is expected to contribute to an increase of the lift force, and to also affect the behavior of the boundary layer. For example, according to Lindenburg[31], the spanwise motion of separated flow gives an additional negative pressure on the airfoil surface,

setting up a negative chordwise pressure gradient which would have a stabilizing effect on the boundary layer. This motion of the separated flow would further make the pressure in the separated area smaller, giving a higher normal force on the airfoil. Corten[19] explains qualitatively the delaying effect on stall of the radially moving separated flow by the fact that it results in attached flow at larger radial positions, while Harris[32] suggested similarly from studying oblique inflow that the transportation of the separated area to larger spanwise locations has an increasing effect on the lift.

These are only a few notions about the possible effects of the presence of radial flow following from the rotation of the blades. Other rotational effects exist, and together with them, many different interpretations on their consequences on the separation of the boundary layer. It was tried here to present the general ideas involved in the phenomenon of stall delay. These ideas are studied further in the two first articles below that present different ways to look at this phenomenon and to model it, and that analyze it in greater detail.

5. RESULTS

5.1. **CONFERENCE ARTICLE no 1** : A study on different stall delay models using a prescribed wake vortex scheme and NREL phase VI experiment data

A Study on Different Stall Delay Models Using a Prescribed Wake Vortex Scheme and NREL Phase VI Experiment

Simon-Philippe Breton*
Department of Civil and Transport Engineering, Norwegian University of Science and Technology, 7491 Trondheim, Norway

Frank N. Coton
Department of Aerospace Engineering, University of Glasgow, Glasgow G128QQ, UK

Geir Moe
Department of Civil and Transport Engineering, Norwegian University of Science and Technology, 7491 Trondheim, Norway

Abstract

A prescribed wake model named HAWTDAWG is used in this study. It is a lifting line model in which the blades are replaced by a line of bound vorticity, and the wake is modelled by a lattice of vortex filaments, whose strengths are based on blade sectional aerodynamic coefficients, usually taken from 2D wind tunnel experiments. Five different stall delay models are incorporated in this model, namely those of Bak et al., Snel et al., Corrigan and Schillings, Du and Selig, and Chaviaropoulos and Hansen. To our knowledge, a study of the proposed stall delay models has never been made with a lifting line, prescribed wake model. In contrast to a code based on the blade element momentum method, the present vortex wake scheme models the wake behind the rotor and its induced effect, providing more detailed information that can shed light on the stall delay phenomenon. Results show that the use of corrected aerodynamic data from the different stall delay models generally leads to an overprediction of the thrust and power for wind speeds above 10 m/s, and of the loads, mostly near the root. The tangential force coefficient for wind velocities above 10 m/s is especially overpredicted over more than half the blade, while it was quite accurately predicted using 2D airfoil data. The stall delay models studied all lead to inaccuracies in some situations in their prediction of three-dimensional flow effects. The present work identifies deficiencies of current correction schemes and provides a basis to develop improved correction models.

*e-mail : simon.breton@ntnu.no, phone:+(47) 73594823, fax: (+47) 73 59 70 21

I. INTRODUCTION

The phenomenon of stall is of very complicated nature, and has for many years captured the attention of several researchers in the helicopter and wind energy aerodynamic fields. A good understanding of this phenomenon is necessary for accurate predictions of the loads on helicopter wings and wind turbine blades. The use of 2D aerodynamic coefficients when simulating a rotating wind turbine results in an underprediction of the blade loads in stalled conditions. This is due to 3D rotational effects that cause the phenomenon of stall to appear at higher angles of attack than it would in a non rotating configuration. Most conventional prediction schemes rely on dividing the turbine blades into a series of spanwise aerodynamically independent sections and so the 2D coefficients have to be corrected for this so-called stall delay. This key issue for the modelling of wind turbines has been addressed by many authors, who proposed different correction models. In this work, five different existing correction models are presented and tested with the help of a lifting line, prescribed wake vortex scheme, under steady inflow conditions. Forces along the blade as well as power and thrust are computed, based on these models, and are compared to the very reliable NREL phase VI experiment data [1]. Discrepancies found to varying extent when applying the models suggest that further work is needed to better model this phenomenon.

II. METHODOLOGY

A. NREL Phase VI Experiment

In this work comparison with experimental data measured on a two-bladed 10.1-meter diameter wind turbine was made. These test series were run in the NASA Ames wind tunnel for NREL and are refered to as the NREL Unsteady Aerodynamics phase VI experiment [1]. The turbine used was stall regulated, its blades were twisted and tapered, and the sectional geometry was that of the S809 airfoil. Measurements were performed in a flow with less than 1 % turbulence, and the data obtained are arguably the most reliable and comprehensive available to this day. Tests were performed in the downwind and upwind configurations, for a wide range of yaw angles, wind speeds, cone and pitch angles, at a constant rotational speed of 71.6 rpm. We will be concentrating here on the upwind baseline configuration, with a zero yaw angle, in which the loading was almost uniform for every azimuth angle. Such conditions are optimal to isolate the phenomenon of stall delay that we suggest to study here. They are then also ideal to perform tests on different existing stall delay models. This configuration also has zero degree cone angle, and a global pitch of three degrees, defined as the angle between the chord at the tip of the blade and the rotational plane. One of the blades was equipped with pressure taps distributed around the airfoil section at 22 different positions, more concentrated near the leading edge of the section to render a better resolution in this more active region of pressure distribution. Such a pressure tap distribution was present at five different locations on the blade, namely at the 30%, 47%, 63%, 80% and 95% spanwise positions. Aerodynamic force coefficients at a particular radial station could then be found by integrating the measured pressure distribution around the corresponding airfoil section. In Fig. 1 we show the convention used for the different coefficients and angles studied. As no cone angle was used in the studied configuration, all the quantities seen in this figure are in the same plane. We will also be looking at the measured thrust and power from this test series. The former is defined normal to the plane of rotation, and it was found from integration of the thrust force along the blade, while the power was found from the measured low speed shaft torque multiplied by the rotational velocity.

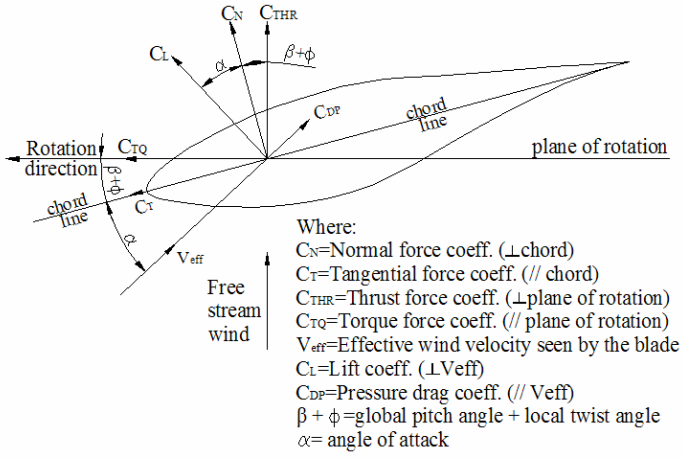

Fig. 1. Section of the blade: convention on angles and aerodynamic coefficients used. ∟: normal to, //: parallel to.

B. The HAWTDAWG model

The HAWTDAWG model is a prescribed wake, lifting line code based on vortex theory. In this code, the blade is modeled as elements which are represented as a line of bound vorticity lying along the blade quarter chord line, representing the loading on the blade. If the bound vorticity is changing from one element to the next, trailing vorticity is introduced to ensure conservation of circulation, in agreement with the theorem of Helmoltz [2]. This trailing vorticity is

modeled as series of straight-line vortex filaments progressing downstream of the trailing edge of the blade. Shed vorticity, which can also be modeled by this code to account for time-varying bound vorticity, will not be of importance here, because of our study of head-on flow only for which there is negligible unsteadiness in the incoming flow. Prescription functions, developed using a free/prescribed wake scheme [3], are used to specify the wake geometry, avoiding the calculation of self induced velocities in the wake. An initial estimate of the induced velocity distribution along the blade is found from blade element momentum (BEM) theory, from which the effective velocity, and thereafter, the angle of attack distribution, are found. Airfoil aerodynamic data, consisting of the lift coefficient versus angle of attack, is then used to find the lift corresponding to the computed angles of attack. The Kutta-Jukowsky [4] law is finally used to find the bound vorticity corresponding to this lift value. The induced velocity distribution, along with the prescription functions, is used to develop the wake shape, onto which the trailing vorticity is distributed. The Biot-Savart law [5] is thereafter used to find the velocities induced by the wake on the blades. The same scheme as before is then used, but now using the new induced velocity distribution from vortex theory. Iterations are performed until global convergence of the wake shape with the lift distribution is obtained. The angle of attack distribution is finally invoked, along with aerodynamic airfoil data in the form of lift and drag coefficients as a function of angle of attack, to find the normal and tangential force coefficients on the blades (see Fig.1). The use of reliable airfoil data is thus seen to be vital in order to obtain accurate simulation results. The airfoil data used here were measured in a wind tunnel at Delft University of Technology [1] (DUT) at a Reynolds number of $1x10^6$, which corresponds best to the tests performed in the NREL wind tunnel, as shown by Coton et al. [6], who studied the use of different available airfoil datasets. For higher angles of attack than supplied by the available measurements, data measured on a NACA 0012 blade up to 180 degrees were used [7], relying on the premise that the performance of an aerofoil is shape insensitive once it goes into the bluff body state. This vortex theory based code is ideally suited for a study of different stall delay models that intend to correct the airfoil data for three-dimensional effects. It does not for example depend on the use of tip or root loss models, because the effect of the tip and root vortices is already modeled by the wake induction effect. It can be used to study stall delay effects, as well as possibly tip and root loss effects, on the airfoil data itself. Airfoil data corrected for these effects could then be used in other vortex wake codes, or in BEM method codes without the need of tip or root loss models [8].

C. Existing correction models

Five different models to correct the airfoil characteristics for stall delay, including a wide range of different assumptions, are studied with the use of the present vortex wake lifting line model. The first three models studied, the ones by Snel et al. [9], Chaviaropoulos and Hansen [10], and Raj [11], correct the lift and drag coefficients C_l and C_d for 3D effects in the following way:

$$\begin{aligned} C_{l,3D} &= C_{l,2D} + g_{Cl}\Delta C_l \\ C_{d,3D} &= C_{d,2D} + g_{Cd}\Delta C_d \end{aligned} \tag{1}$$

where g_{Cl} and g_{Cd} are functions inherent in each correction model, and ΔC_l and ΔC_d are the difference between the the C_l and C_d that would be obtained if the flow did not separate (taken here respectively as $C_l=2\pi*(\alpha- \alpha_{lift=0})$, and $C_d=C_d(\alpha=0)$) and the C_l and C_d measured in a 2D configuration (i.e. $C_{l,2D}$ and $C_{d,2D}$).

Snel et al. [9] proposed a model following from the solution of a simplified form of the 3D boundary layer equations on a rotating blade, which reads as

$$g_{Cl} = 3(c/r)^2 , \tag{2}$$

where c and r are respectively the local chord and radius. No correction to the drag coefficient was proposed.

Chaviaropoulos and Hansen [10] used for their study of the stall delay phenomenon a quasi-3D model based on the solution of a system of simplified equations derived by integrating the 3D incompressible Navier-Stokes equations in the radial direction, from which they developed the following semi-empirical model to correct for 3D rotational effects:

$$\begin{aligned} g_{Cl} &= a(c/r)^h \cos^n(\phi) \\ g_{Cd} &= a(c/r)^h \cos^n(\phi) \end{aligned} \tag{3}$$

where ϕ is the local twist angle. The values of the constants given by the authors as a=2.2, h=1, and n=4 will be used here.

Du and Selig's stall delay model [12] is based on the analysis of the 3D integral boundary layer equations on a rotating blade, as an extension of the work of Snel et al. [9]. Their model reads as:

$$g_{Cl} = \frac{1}{2\pi}\left[\frac{1.6(c/r)}{0.1267}\frac{a-(c/r)^{\frac{d}{\Lambda}\frac{R}{r}}}{b+(c/r)^{\frac{d}{\Lambda}\frac{R}{r}}}-1\right]$$
$$g_{Cd} = \frac{1}{2\pi}\left[\frac{1.6(c/r)}{0.1267}\frac{a-(c/r)^{\frac{d}{2\Lambda}\frac{R}{r}}}{b+(c/r)^{\frac{d}{\Lambda}\frac{R}{r}}}-1\right] \quad (4)$$

where $\Lambda = \Omega R/\sqrt{V_0{}^2+(\Omega R)^2}$ is a modified tip speed ratio, with V_0 the incoming wind speed, Ω the rotational velocity, and R the blade span. The constants a, b, and d given as 1 by the author will be used here.

Bak et al. [13] have very recently proposed a model based on the analysis of the difference between the pressure distribution on a rotating and a non-rotating blade. The phase VI NREL test turbine was used in this process, along with airfoil data measured in a 2D configuration in a wind tunnel. This difference is expressed via the quantity ΔC_p representing the contribution from the 3D effects to the pressure difference between the suction and pressure sides of the airfoil. This quantity is modelled as the product of a shape function and an amplification function of the pressure differences. The shape factor is found from an analysis of the shape of ΔC_p from measurements at the 30% span location. The resulting model for ΔC_p is given as

$$\Delta Cp = \frac{5}{2}(1-\frac{x}{c})^2(\frac{\alpha-\alpha_{f=1}}{\alpha_{f=0}-\alpha_{f=1}})^2\sqrt{1+\left(\frac{R}{r}\right)^2}\left(\frac{c}{r}\right)/(1+\tan^2(\alpha+\theta)), \quad (5)$$

where x/c is the normalized chordwise position, α is the angle of attack and $\alpha_{f=1}$ and $\alpha_{f=0}$ are respectively the angles of attack where the flow around the airfoil is just about to separate, and just fully separated. ΔC_n and ΔC_t are then found by integration of this factor along the different blade airfoil geometries, and are added to the 2D values to find $C_{n,3D}$ and $C_{t,3D}$, the 3D corrected values of the normal and tangential force coefficients. The corrected airfoil coefficients $C_{l,3D}$ and $C_{d,3D}$ are finally found from

$$C_{l,3D} = C_{n,3D}\cos(\alpha)+C_{t,3D}\sin(\alpha)$$
$$C_{d,3D} = C_{n,3D}\sin(\alpha)-C_{t,3D}\cos(\alpha) \quad (6)$$

Corrigan and Schillings [14] developed their model starting from the analysis of Banks and Gadd [15], based on the pressure gradients in the boundary layer. Their idea was that the findings of Banks and Gadd could be used to develop a shape function for stall delay, formulated in terms of the angular position of the separation point. The delay of stall was finally expressed as a shift in angle of attack:

$$\Delta\alpha = \left(\alpha_{C_{l_{\max}}}-\alpha_0\right)\left[\left(\frac{Kc/r}{0.136}\right)^n-1\right], \quad (7)$$

where $\alpha_{C_{l_{\max}}}$ is the angle of attack corresponding to the first maximum of the lift coefficient, and K is the non dimensional linear adverse velocity gradient used in the formulation of the model. The constant n is related to the intensity of the rotational effects, and is suggested to be chosen in agreement with test data. Corrigan and Schillings recommend using a value between 0.8 and 1.6, and mention that using n=1 was satisfactory in many cases. Tangler and Selig [16] also used n=1 in this model, and this is the value to be used herein. The whole airfoil table of non-rotating lift and drag coefficients is to be shifted over this stall delay angle $\Delta\alpha$, where the lift coefficient is further corrected in the following way:

$$C_{l,3D}(\alpha+\Delta\alpha) = C_{l,2D}(\alpha)+\partial C_{l,pot}/\partial\alpha\cdot\Delta\alpha, \quad (8)$$

where $\partial C_{l,pot}/\partial\alpha$ is the slope of the potential theory lift curve. Corrigan and Schillings suggested to apply this model up to a 75% spanwise position, above which they suggested that stall delay effects should not be present.

III. RESULTS

Fig. 2 shows an example of the results obtained from applying the different correction models to the 2D airfoil data for conditions equivalent to the 30% of span location of the NREL blade for a tip speed ratio of 1.5. The results presented in this figure are obtained by simply correcting the 2D data using the various correction formulae. There are considerable differences between the predictions from the different models. Looking first at the lift coefficient in Fig. 2(a), we see that the model from Corrigan and Schillings is the one that has the least effect. The models from Snel et al., Du

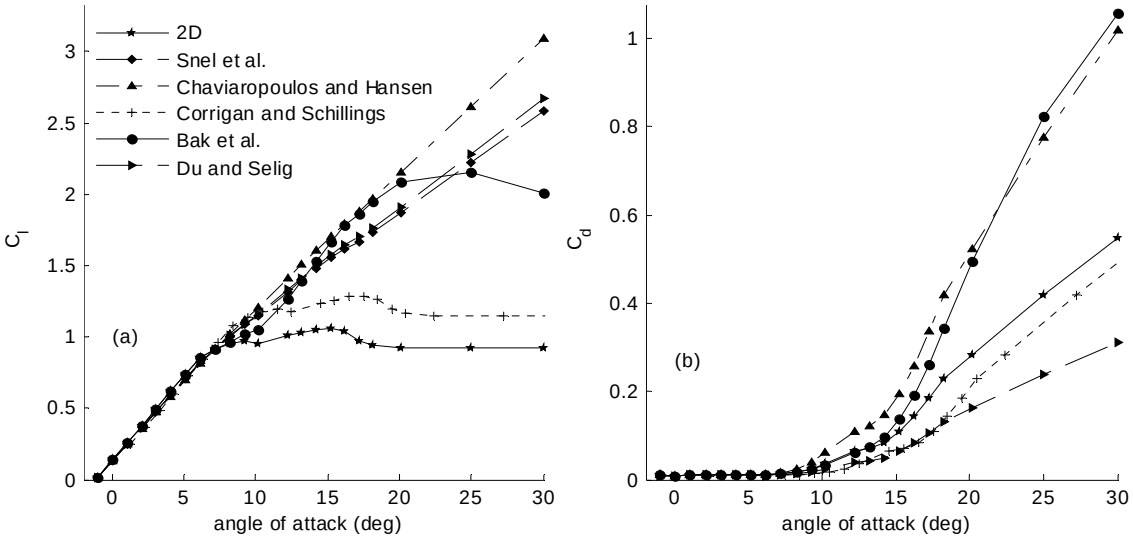

Fig. 2. Lift (a) and drag (b) coefficients as a function of angle of attack measured at DUT in 2D tests of blade sections, and corrected with different stall delay models at the 30% spanwise position.

and Selig, and Chaviaropoulos and Hansen, lead to the largest corrections overall. Also in these cases the lift coefficients continue to increase monotonically above 30 degrees angle of attack. The correction following the model of Bak et al. is also quite significant and produces a maximum lift coefficient at 20 degrees angle of attack. As seen in Fig. 2(b), the correction to the drag coefficient from the model of Corrigan and Schillings is also the smallest one. Note that a decrease of the drag coefficient is predicted for this model and for Du and Selig's model. The models of Chaviaropoulos and Hansen and Bak et al. produce very high values of drag coefficient at high angles of attack compared with the original two-dimensional data. It should be noted here that the different models would also correct the airfoil data at spanwise

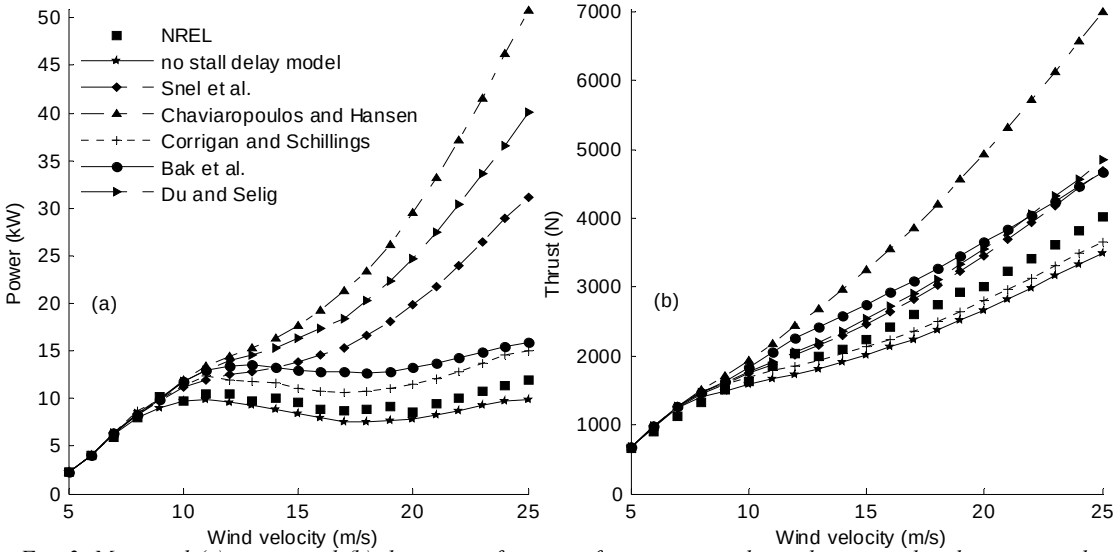

Fig. 3. Measured (a) power and (b) thrust as a function of incoming wind speed compared with power predicted from HAWTDAWG with and without different stall delay models.

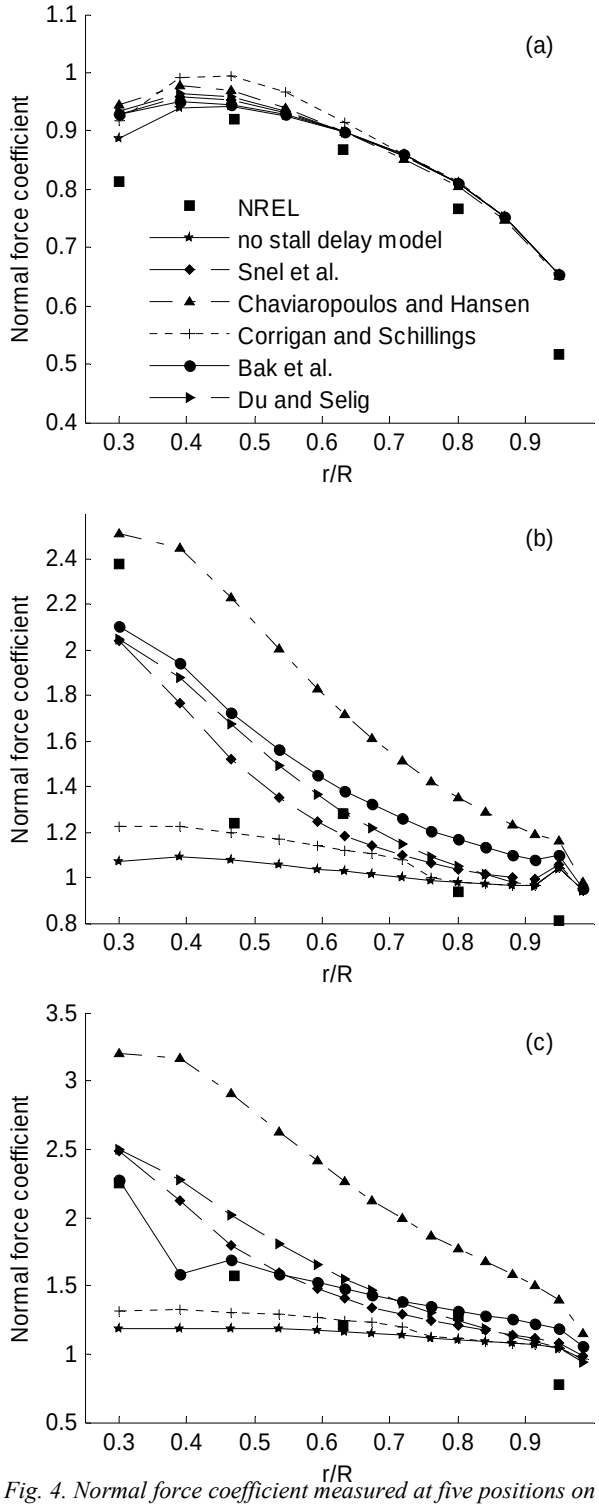

Fig. 4. Normal force coefficient measured at five positions on the blade compared with normal force coefficient predicted from HAWTDAWG with and without different stall delay models, for incoming wind velocities of (a) 7m/s, (b) 16m/s, (c) 25m/s.

positions further outboard on the blade but to a lesser extent than the case shown here. In some cases, the formulae produce corrections right out to the tip of the blade.

Figures 3(a) and 3(b) show the effects of the various correction schemes on the power and thrust predicted by the HAWTDAWG model. Looking at these figures, we see that good agreement is obtained up to about 10 m/s in the prediction of the power and thrust, between all the stall delay models, the uncorrected case and the NREL measured data. Thus, the stall delay models are seen to have only a minor influence at these wind speeds. At higher wind speeds, the use of 2D airfoil data leads to an underprediction of these two quantities, while application of the different models generally leads to overpredictions and great disparities in the results. Looking at the power, we see that the correction models from Snel et al., Du and Selig, and Chaviaropoulos and Hansen, lead to the largest overpredictions. The predictions from the models of Bak et al., and Corrigan and Schillings, are significantly closer to the NREL data. The thrust is also significantly overpredicted by these three first models. However, in this case, the overprediction due to the models of Snel et al. and Du and Selig is significantly less than that from Chaviaropoulos and Hansen's model, and is comparable to Bak et al.'s model. Thrust is uniquely underpredicted by the model of Corrigan and Schillings from about 12 m/s upwards. The power and thrust are quantities representing integrated forces along the blade span. It is of great interest to investigate the local distribution of forces. This is done in Figs. 4 and 5 by comparing the predictions with the integrated loads from NREL's pressure measurements at five different positions on the blade.

In Fig. 4(a), it is seen that the normal force coefficient is quite well predicted at low wind speed along the blade by all the stall-delay models and for the uncorrected case except for a small overprediction near the root, and a larger overprediction near the tip. The tangential force prediction is also very good at low wind speed in all cases, even near the tip and root, as seen in Fig. 5(a). This changes with increasing wind speed which produces a growing disagreement with the measured data. The normal force coefficient at 16 m/s, in Fig. 4(b), is severely overpredicted by the model of Chaviaropoulos and Hansen over most of the span despite capturing the measured value well near the root. As mentioned above, all of the

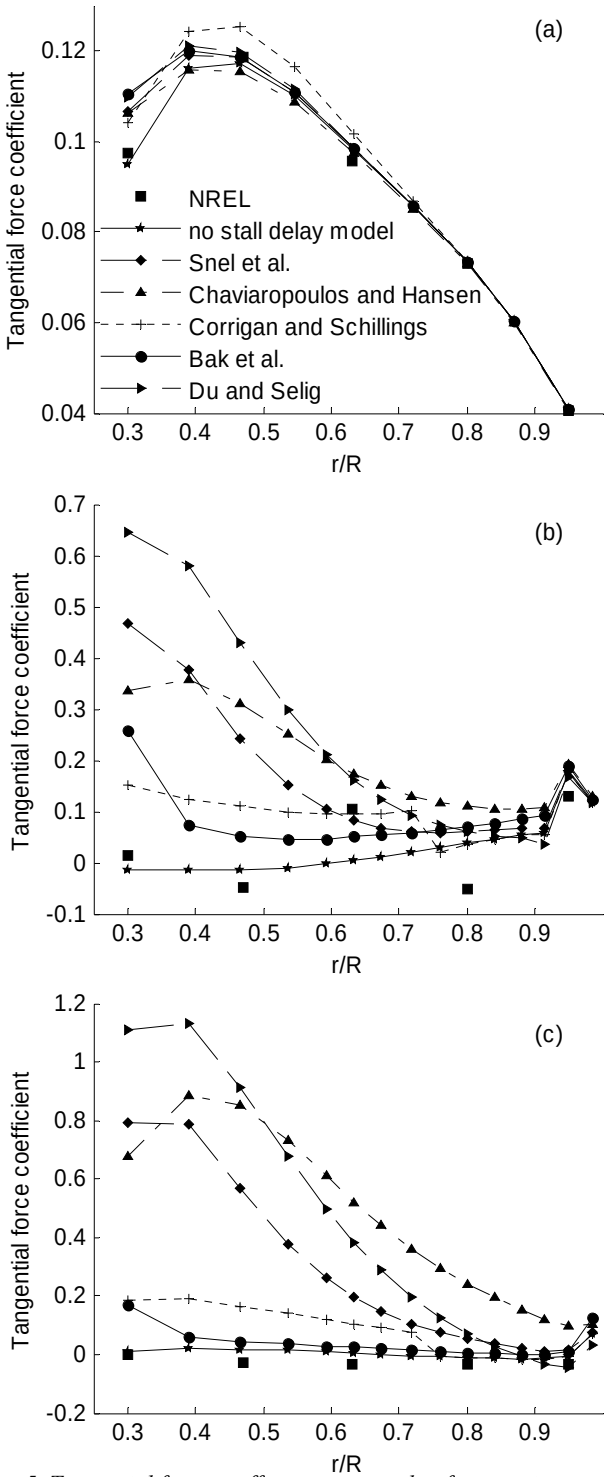

Fig. 5. Tangential force coefficient measured at five positions on the blade compared with tangential force coefficient predicted from HAWTDAWG with and without different stall delay models, for incoming wind velocities of (a) 7m/s, (b) 16m/s, (c) 25m/s.

models overpredict the normal force near the tip, but the uncorrected predictions underpredict the normal force inboard of 80% of span. Conversely, the models of Snel et al., Du and Selig and Bak et al. give an overprediction on the inboard half of the blade, except very close to the root, where the modelled force coefficients are too small. For this case, Corrigan and Schillings' model produces an underprediction inboard of the 80% of span position. At 25m/s, in Fig. 4(c), a general overprediction is also seen near the tip. Chaviaropoulos and Hansen's model again results in a significant overprediction along the whole blade, while Snel et al.'s and Du and Selig's models lead to an overestimation over a shorter stretch of the blade, i.e., inboard of the 80% spanwise position. Bak et al.'s model seems to result in the best agreement, while underprediction results from using Corrigan's model inboard of 60% span.

While the prediction using 2D data was quite good for the tangential force coefficient at 16 and 25m/s, as seen in Fig. 5(b) and 5(c), the use of all the stall delay models led to an overprediction over at least the inboard half of the blade, with the highest overprediction coming from Du and Selig's, Snel et al., and Chaviaropoulos and Hansen's models. At 25 m/s, this overprediction is seen inboard of the 80% spanwise position for these three models. A small overprediction is seen from the use of all the models at the 95% spanwise position at 16 m/s, while the agreement is quite good at 25 m/s, except for Chaviaropoulos and Hansen's model which produces an overprediction. Let us note finally that the curve associated with the 2D predictions, as well as those associated with all the stall delay models, show a tangential force coefficient going up near the tip of the blade at 25 m/s. This tendency in the predictions was actually observed for wind speeds of 17 m/s or more. The simulated normal force was also seen to increase near the tip of the blade from wind speeds of 17 m/s to 24 m/s.

IV. DISCUSSION

The spread of the corrected airfoil data seen in Fig. 2 follows from the widely varying assumptions related to each model used. The disparity in the predictions in Figs. 3 to 5 illustrates the important effects of the airfoil data and, more importantly, of the different models on the simulation results. The underprediction of the simulated thrust and power seen in Figs. 3(a) and 3(b) when using 2D airfoil data was expected from theory, and

shows that 3D rotational effects should be included in wind turbine load simulations. The good agreement seen between the different simulation results and NREL measured data at low wind speed, where stall delay is not of importance, is a sign pointing towards reliability of the code used. The deterioration of the level of agreement, appearing at higher wind speeds, indicates incorrect modelling of the stall delay phenomenon, which then takes on more importance under these conditions. The general overprediction of power seen in Fig. 3(a) shows that the different models over-correct for this effect. It is interesting that the models that produced the largest overpredictions were those depending on the factor ΔC_l. This is likely to be due to this factor giving too large a correction at high angles of attack because of its dependency on the term $2\ \pi^*\alpha$, which grows linearly with angle of attack. The general overprediction of thrust observed in Fig. 3(b) is another indicator that the effect of stall delay is overestimated in a similar way by the different models, with the exception of the model of Corrigan and Schillings. However, it should be noted, as seen in Fig.1, that the thrust value is closely related to the normal force coefficient, whereas the power value is associated more with the tangential force coefficient. The fact that the tangential force coefficient was generally overpredicted more than the normal force coefficient explains why the power was also generally more overestimated than the thrust. It also explains why the models that overpredict the tangential force the most are also the ones that overestimate the power the most, and similarly concerning the normal force coefficient and the thrust. Particularly, the unique underprediction of the thrust resulting from the use of Corrigan and Schillings' model can be related to the important underprediction of the normal force that was observed on the inboard part of the blade with this model.

The good agreement seen between the predictions and measured values of the normal and tangential force coefficients observed in Fig. 4(a) and Fig. 5(a) at low wind speed points again towards reliability of the code used, this time at the local level. The behavior observed near the tip in Fig. 4(a) indicates that special attention is needed in this region. Once again, the fact that the disagreement between the measured data and the models grows with increasing wind speed points towards an unsatisfactory modelling of the stall delay phenomenon by the different models used. It was seen that some models predict either the normal or the tangential force coefficient in a reasonably accurate way, but all the models were unable to capture both behaviors at the same time. The most significant overpredictions of the local loads were also obtained using models that depend on the factor ΔC_l .The general overprediction of the force coefficients observed near the tip, even at low wind speed, and in the 2D case, suggests that a special correction might be needed in that region. The current modeling of an increase of the lift coefficient due to stall delay effects in the tip region by most models goes against recent studies [17,8] claiming that the lift should rather go down in this region. A stall delay model that was recently proposed by Lindenburg [18], and that incorporates a special correction model near the tip to account for a decreasing lift, would be of great interest to test against the current models. Another reason to look at this model in more detail is that it simulates the stall delay phenomenon using a new way of modeling the centrifugal pumping mechanism [19]. Let us note that Corrigan and Schillings' suggestion of not applying their model above the 75% spanwise position seemed justified, aligning their results with the 2D case in this region, and thus avoiding a significant overprediction at the tip. The increase of the tangential and normal forces near the tip of the blade is one more indication that special care needs to be taken in this region. The reason behind such a result can be simply explained. The angle of attack is expected to go down near the tip of the blade because of the effect of the tip vortex. If the geometric angle of attack near the tip is above the 2D stall angle then a reduction in the effective incidence will result in an increase in lift. Further inboard, where the downwash is less, the effective angle will remain above the stalling incidence and will be associated with a lower lift coefficient. This result may not be physically correct and might be avoided by using a special correction model near the tip such as the one proposed by Lindenburg [18].

The larger overprediction of the loads produced by the model of Chaviaropoulos and Hansen, when compared to the model of Snel et al., to which it is very similar, is due to the smaller exponent used for the term *c/r* in the former case. The higher exponent used in the model of Snel et al. has the important effect of decreasing the correction when moving away from the root. The relatively good agreement near the blade root of the results obtained from applying the model of Bak et al. is expected to be due to the fact that experimental data at this position were used in the development of this model. Problems observed locally away from the root resulted in discrepancies in predictions of the power and thrust. Recent studies [17, 8] suggested an increase of the drag coefficient arising from rotational effects. It is expected that predictions based on Corrigan and Schillings' and Du and Selig's models could be improved if they predicted a rise of the drag coefficient instead of the current decrease. The Snel et al. model could also benefit from an increase of the drag coefficient which is currently not corrected for stall delay effects. Less power would, for example, be predicted if the drag coefficients predicted by the methods were higher. In this respect the model developed by Raj [11] from Du and Selig's model [12] may provide an improvement over the latter. This model predicts an increase in the drag coefficient resulting from rotational effects and allows more flexibility in the drag and lift coefficient corrections. It also employs a cut-off angle at which stall delay corrections are no longer applied. The present results suggest that one possible way in which the predictions from the three models depending on the factor ΔC_l could be improved would be to stop the correction at a certain angle of attack, following the idea from Raj, or to somehow limit the rise of this factor for increasing angles of attack.

V. CONCLUSION

Different models intended to correct for stall delay were tested in a lifting line, prescribed wake vortex scheme. Comparisons were performed with very reliable wind tunnel data measured by NREL. The models were shown to exhibit inaccuracies in their modelling of the stall delay phenomenon. An overprediction of the loads was generally obtained, most significantly for models depending on a linear relation of lift coefficient with the angle of attack. It was suggested that applying these models only up to a certain angle of attack, following the method Raj, may produce better results. It was also suggested that this method may provide an improvement over the model from Du and Selig. Special attention was shown to be needed near the tip of the blade, where the loads were often overpredicted. A new correction model by Lindenburg, including among other things a special reduction of lift in this region, was suggested to be considered in a further study. Possible improvements concerning the use of the different models were also suggested. In future work it would be interesting to compare simulation results with NREL measurements of the root flap bending moment instead of the thrust, because the former was measured directly at the root of the blade, as opposed to the latter which was estimated from pressure measurements performed at five different positions on the blade. Much work is, however, still needed in order to reach a satisfactory understanding of the complex phenomenon of stall delay.

REFERENCES

[1] Hand MM, Simms DA, Fingersh LJ, Jager DW, Cotrell JR, Schreck S, Larwood, SM. *Unsteady Aerodynamics Experiment Phase VI: Wind Tunnel Test Configurations and Available Data Campaigns*, *NREL/TP–500-29955*; National Renewable Energy Laboratory: Golden, CO, 2001.

[2] Bertin JJ, Smith ML, *Aerodymamics for Engineers*; Prentice-Hall Inc.: Upper Saddle River, USA, 1998; 266-267.

[3] Robison DJ, Coton FN, Galbraith RAMcD, Vezza M. Application of a prescribed wake aerodynamic prediction scheme to horizontal axis wind turbine in axial flow. Wind Engineering 1995; **19**:41-51.

[4] Bertin, JJ, Smith ML, *Aerodymamics for Engineers*; Prentice-Hall Inc.: Upper Saddle River, USA, 1998; 103-104.

[5] Bertin JJ, Smith ML, *Aerodymamics for Engineers*; Prentice-Hall Inc.: Upper Saddle River, USA, 1998; 294.

[6] Coton FN, Wang T, Galbraith RAM, An Examination of Key Aerodynamic Modelling Issues Raised by the NREL Blind Comparison, *Wind Energy* 2002; **5**:199-212.

[7] Sheldahl RE, Klimas PC. *Aerodynamic Characteristics of Seven Symmetrical Airfoil Sections through 180-degree Angle of Attack For Use in Aerodynamic Analysis of Vertical Axis Wind Turbines, Sandia Report, SAND80-2114 UC-261*; Sandia National Laboratories: Albuquerque, USA, 1981.

[8] Johansen J., Sørensen NN, Aerofoil Characteristics from 3D CFD Rotor Computations, *Wind Energy* 2004; **7**:283-294.

[9] Snel H, Houwink R, van Bussel GJW, Bruining A, Sectional Prediction of 3D Effects for Stalled Flow on Rotating Blades and Comparison with Measurements, *Proc. European Community Wind Energy Conference*: Lübeck-Travemünde, Germany, 1993; 395-399.

[10] Chaviaropoulos PK, Hansen MOL, Investigating Three-Dimensional and Rotational Effects on Wind Turbine Blades by Means of a Quasi-3D Navier Stokes Solver, *J. Fluids Engineering* 2000; **122**:330-336.

[11] Raj, NV, *An Improved Semi-Empirical Model for 3-D Post-Stall Effects in Horizontal Axis Wind Turbines,* Master of Science Thesis in Aeronautical and Astronautical Engineering, University of Illinois at Urhana-Champaign: Urhana, IL, 2000

[12] Du Z, Selig MS, A 3-D Stall-Delay Model for Horizontal Axis Wind Turbine Performance Prediction, AIAA-98-0021.

[13] Bak C, Johansen J, Andersen PB, Three-Dimensional Corrections of Airfoil Characteristics Based on Pressure Distributions, *Proceedings of the European Wind Energy Conference*: Athens, Greece, 2006.

[14] Corrigan, JJ, Schilling JJ, Empirical Model for Stall Delay Due to Rotation, *Proceedings of the American Helicopter Society Aeromechanics Specialists Conference*: San Francisco, CA, 1994.

[15] Banks, WHH, Gadd GE, Delaying Effect of Rotation on Laminar Separation, *AIAA Journal* 1963; **1**:941-942.

[16] Tangler JL, Selig MS, An evaluation of an empirical model for stall delay due to rotation for HAWTs, *Proceedings of Windpower '97*: Austin, TX, 1997; 87-96.

[17] Sørensen NN, Michelsen JA, Schreck S, Navier-Stokes Predictions of the NREL Phase VI Rotor in the NASA Ames 80 ftx 120 ft Wind Tunnel, Wind Energy 2002; **5**:151-169.

[18] Lindenburg C, *Investigation into Rotor Blade Aerodynamics*, *ECN-C--03-025*; ECN: Petten, Netherlands, 2003.

[19] Eggers AJ, Digumarthi R, Approximate Scaling of Rotational Effects of Mean Aerodynamic Moments and Power Generated by the Combined Experiment Rotor Blades Operating in Deep-Stalled Flow, *11-th ASME Wind Energy Symposium*; Houston, TX, 1992; pp.33-43.

5.2. **JOURNAL ARTICLE no 1** : A study on rotational effects and different stall delay models using a prescribed wake vortex scheme and NREL phase VI experiment data

Is not included due to copyright

5.3. <u>JOURNAL ARTICLE no 2</u> : Assessment of motions, moments and forces in the NREL NASA Ames wind tunnel tests

Is not included due to copyright

5.4. <u>JOURNAL ARTICLE no 3</u> : Status, plans and technologies for offshore wind turbines in Europe and North America

Status, Plans and Technologies for Offshore Wind Turbines in Europe and North America

Simon-Philippe Breton, Geir Moe
Department of Civil and Transport Engineering, Norwegian University of Science and Technology, 7491 Trondheim, Norway

Abstract

The worldwide demand for renewable energy is increasing rapidly because of the climate problem, and also because oil resources are limited. Wind energy appears as a clean and good solution to cope with a great part of this energy demand. In Denmark for example, 20% of the electricity is produced from wind, and plans are towards reaching 50%. As space is becoming scarce for the installation of onshore wind turbines, offshore wind energy, when possible, seems as a good alternative. This work describes, for Europe and North America, the potential for offshore wind energy, the current status of this technology, and existing plans for the development of offshore wind parks. It also presents existing as well as promising new solutions for offshore wind energy.

I. Introduction

Increasing oil prices and energy demand combined with a general acceptance that man made global warming is occurring intensifies the search for new energy solutions. Wind energy is a clean and inexpensive alternative, and as space is quickly becoming scarce for the installation of onshore wind turbines, offshore wind energy has become an increasingly attractive option due to the enormous energy potential associated with the vast offshore areas. Optimal solutions for offshore wind energy are expected to differ from its onshore counterpart, and successful adapted solutions might result in great reductions of costs, making this form of energy more competitive and its deployment more important in the coming years. As such, it is expected to be the next big step in wind energy development. This technology has up to now been exclusive to Europe, but North America, where conditions differ from those of the existing European offshore wind parks, is now appearing as an important upcoming player.

II. Advantages and challenges compared with onshore

There are many advantages to offshore wind energy, compared to its onshore counterpart. Stronger winds offshore imply greater productivity that may offset higher installation and operation costs. Installing wind turbines sufficiently far from the shore can nearly eliminate the issues of visual impact and noise. This makes it possible to use different designs for the turbines, improving their efficiency. This also makes huge areas available for the installation of large wind parks. As transportation and erection are made at sea, there is virtually no limit on the size of the turbines that can be installed, as opposed to limits imposed by road restrictions onshore. Also, offshore wind parks can be installed close to major urban centers, requiring shorter transmission lines to bring this clean energy to these high energy cost markets. Several challenges are however met by offshore wind energy. Higher investments in towers and underwater

cabling are needed, along with a long planning phase including among others environmental, engineering, feasibility, and site-specific studies. Environmental conditions are also more severe offshore. One must deal with wave and current loading, as well as possibly ice loading, and corrosion from salty waters. Access for maintenance and repair is also more difficult offshore. In some areas competition with other marine users will also be a problem.

III. Current status and plans in Europe and North America

The status of offshore wind energy is very different in Europe and North America. At the end of 2006, Europe had operating wind farms in Denmark (398 MW), United Kingdom (304 MW), Ireland (25 MW), Sweden (23.3 MW) and the Netherlands (136 MW). It represented then 1.8% of the installed wind energy, but 3.3% of the wind energy production [1]. Fig. 1 shows a map of the existing and planned wind turbines in North West Europe, where the development has been concentrated up to now.

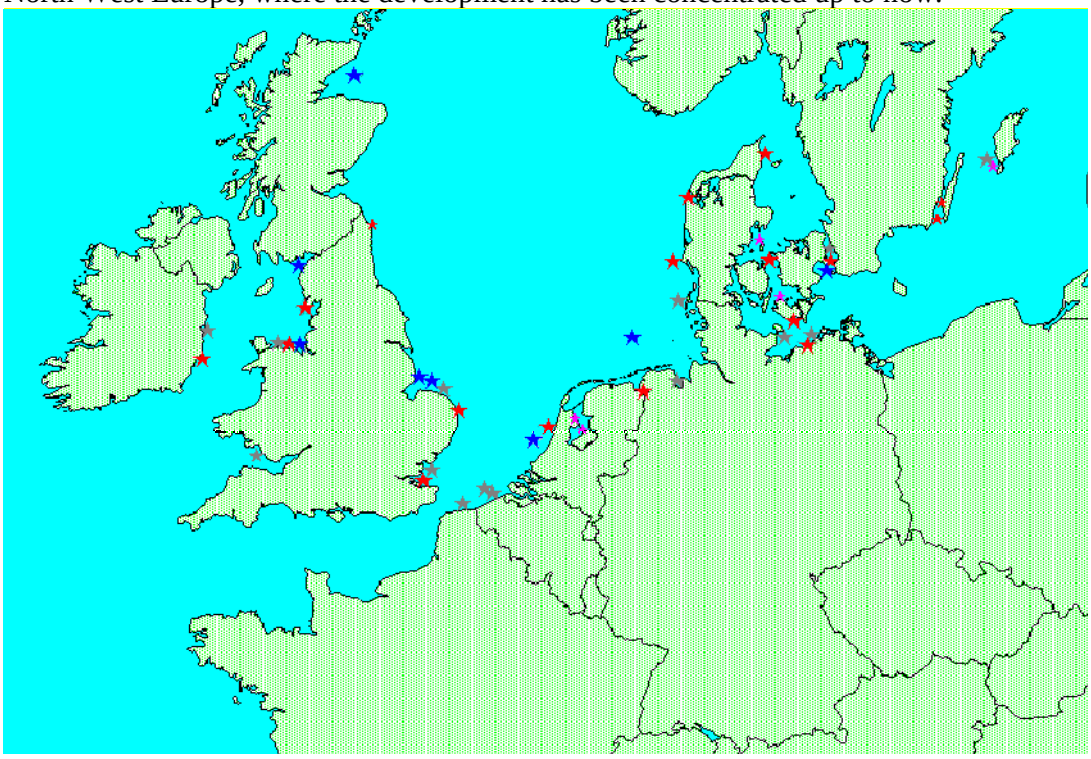

Fig. 1. Existing and planned wind farms in North-West Europe, June 2007 [2]. Red = (built MW turbines), purple=(built small turbines), blue=(under construction), grey=(planned).

Offshore wind energy development is taken very seriously in Europe. In February 2007, it was given high priority when European member states made a firm commitment to increase the total share of renewables in primary energy consumption to 20% by 2020 [3]. The target is to reach 50 GW of offshore wind energy by 2020. This is a progression for the next 13 years that would correspond to the development seen in the onshore sector in the last 13 years [1].

Let us now look at examples of important or upcoming players in the European offshore wind energy market. The key European markets have up to now been Denmark and the UK. Denmark was the pioneer in this field as it built the first offshore wind farm in the world in Vindeby in 1991. It has now eight operating wind farms, including the biggest one in the world, located at Horns Rev in the North sea (Fig. 2), composed of 80 2MW turbines that generate enough power to meet the demand of 150 000 Danish Homes. Wind conditions in this area being exceptional, the production of this wind farm is equal to rated production between 40 and 50% of the year [4]

Fig. 2. Horns Rev offshore wind farm [5].

Two upcoming farms of a capacity of 200 MW each, Horns Rev II and Rødsand, expected to be commissioned 2009/2010, will generate enough energy to power from 350 000 to 400 000 Danish homes, or 4% of the Danish electricity consumption. Wind energy might be able to produce more than 50% of the Danish electricity needs by 2025, and most of the new parks are expected to be located offshore [4]. The UK has five operating wind farms. The development plans are huge, and as of now, leases have been allocated for parks totalling 7200 MW, corresponding to 7% of UK's electricity supply [6]. The UK has also built the demonstration farm called Beatrice [7], in a water depth of 45 m, making it the deepest wind turbine site in the world. Germany has no operating wind farm yet, but it is expected to be a key player in the years to come, as projections from the German Environment Ministry claim a target of 1100 MW by 2010, and from 12000 to 15500 MW by 2020 [8]. Norway does not have an operating offshore wind farm yet, but the company Statkraft is developing plans for a 1000 MW park in water depths of 30 to 60m by 2012 [9], that would make it the deepest wind park in the world. Further developments are planned or under construction off the coasts of the Netherlands, Belgium, France and Spain, where Spain made recently an important move by allowing the construction of offshore parks bigger than 50 MW [10].

North America is still at a planning stage concerning offshore wind energy, as it does not yet have operating offshore wind farms. The potential, however, is enormous. The areas off the US coast within a 50 nautical miles limit represent a potential of 907 GW, which is close the currently installed generating capacity in that country [11]. Potential in the Great Lakes and in the Gulf Coast are not even included in this estimate. 98 GW of this capacity is located in waters shallower than 30 m. Fig. 3 shows the wind off the US coast, compared with the US density of population. A very interesting

correspondence is seen between these two maps, showing the great possibilities regarding offshore wind energy in the US. Canada also has an enormous offshore potential, as seen in Fig. 4 which shows the mean wind speed at 50 m above the ground in Canada and along its shores.

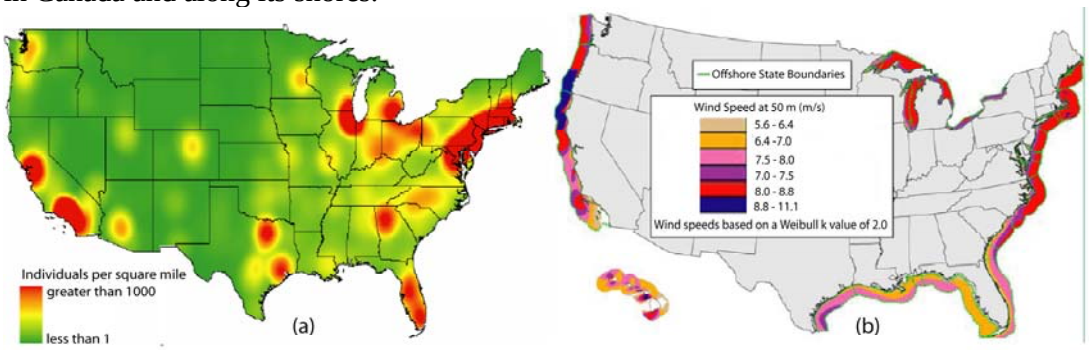

Fig. 3.(a) US population concentration compared with (b) US offshore wind resource. (Adapted from [12]).

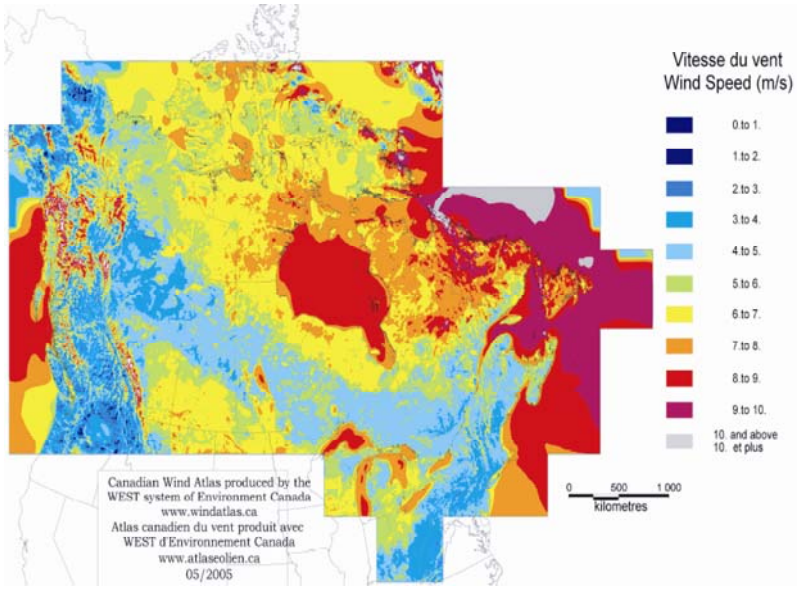

Fig. 4. Mean Wind Speed at 50 m above ground. Horizontal resolution of 5 km [13].

Five important projects are competing to become the first offshore wind park in North America [14]. The Cape Wind project, located off the coast of Cape Cod in the US, would have 130 turbines totalling 420 MW. Construction is expected to begin in 2010. However, problems as regards public acceptance are manifest for this project, and might prevent its realization, and some even say, jeopardize the future of offshore wind energy in the US [15]. The Bluewater Wind project [16], off the coast of Delaware, in the US, would provide this state with 600 MW of clean electricity. Construction and installation are planned from 2010. Construction of the LIPA Offshore wind park [17], in Long Island, US, is expected to begin in 2008. It would be composed of 40 3.6 MW turbines. A project developed by Wind Energy Systems Technologies LLC in the Gulf of Mexico off the coast of Texas is planned to generate 150 MW of wind energy by 2012 [18].

Finally, the construction of the first phase of the Nai Kun project [19], in the Hecate Strait of British Columbia, Canada, is planned to begin in 2009. This first phase of 320 MW would be followed by at least four other phases to reach a total of 1750 MW.

Thus it is seen that Europe has a lead over North America in all facets of offshore wind energy development, e.g. technology, construction, operation, and this is also so for studies of environmental impacts. In 2006 Denmark has for example published an extensive report [4] based on its experience with offshore wind energy, that presents the results of a study of the impact of the Horns Rev and Nysted offshore wind parks on for instance birds and marine life, going all the way from their construction to their operation. One has to have operated an offshore wind park a certain number of years in order to perform such a study, and this is the case with Denmark that has now developed a significant experience in the planning, construction and operation of offshore wind turbines. It is however important to mention that conditions differ significantly between the existing European offshore sites and the North American wind park locations now under consideration, so the technology developed for European conditions are not directly applicable for North America. For example, in North America, most offshore projects are now planned in oceans, which have very different weather conditions than the sheltered, shallow water sites that have up to now been developed in Europe. Stronger wind and larger wave and ice loadings will have to be considered. Offshore wind parks have up to now been installed in waters shallower than 30 m. In North America, much of the potential sites are located in deeper waters, so that new technologies will be required. This is also true for countries like Norway and Portugal where large areas are available in quite deep waters. Let us now look at existing and new solutions for offshore wind energy.

IV. Existing and new solutions

As was recently mentioned in the conclusions of a report by the International Energy Agency, *"Despite significant technological progress in the past, R&D is still needed, especially for larger turbine designs, for future projects of large scale or in deep water"* [20]. Up to now, concerning the turbines themselves, what we have seen is mostly that onshore technology has been used directly under offshore conditions. However, optimal offshore turbine designs are expected to differ from their onshore counterpart. For example, as noise is no longer an important issue provided the turbines are located far enough from the shore, the use of the noisier downwind turbines could be favored. This type of turbine is inherently more stable in the wind, making it possible to use an easier yawing system. Another advantage of this type of turbine compared to an upwind turbine is that the introduction of a cone angle to keep the blades away from the tower results in a centrifugal force that creates a moment at the root opposing the moment due to the thrust force, therefore reducing it, whereas both moments are acting in the same direction in the upwind configuration. A downwind configuration could also permit the use softer and cheaper blades, as they would deflect away from the tower in this configuration, reducing the danger for hitting the tower. More efficient but noisier blades could also be used, as many costly restrictions on the blades have been made in the past years to reduce their noise. For example, studies have shown that loads on the blades could be reduced by the use of high tip speed and reduced blade chord designs

[21]. Significant energy cost reductions could apparently be realized by the use of such designs, where a blade with lower solidity and higher rotational speed is found to perform the same mechanical work more efficiently. Visual impact being less of an issue offshore, reductions in costs could also be made by the use of different designs. Tubular towers, that have been used onshore mostly for esthetic reasons, could be replaced by cheaper truss towers. The smaller importance of visual impact would also make it possible to build bigger turbines, for which new designs could become more optimal. However, bigger is not necessarily better, as was recently discussed in a paper by Moe [22]. Using the principle of geometric similarity, according to which the dimensions of the turbine would all grow in the same proportion, it follows that the mass of the turbine, related to the amount of material it contains, increases faster than the increase in the energy captured, even when a change in velocity with altitude is considered. Moreover, gearboxes can become very expensive as the turbines get bigger and the blades rotate more slowly, so that the gearing ratio increases. However, many factors have to be considered, such as cost increases for the construction materials, and learning curve effects. The latter refers to the fact that it is difficult to compare today's technology regarding bigger turbines with yesterday's concerning smaller turbines, because technology has greatly improved with time, and size effects are difficult to isolate clearly. Thus even if bigger turbines that are being built today may seem cheaper, this might only follow from an improvement in the techniques used, that could also benefit smaller turbines today. Therefore, one has to be careful as to how much can be saved by continuing to increase the size of the turbines.

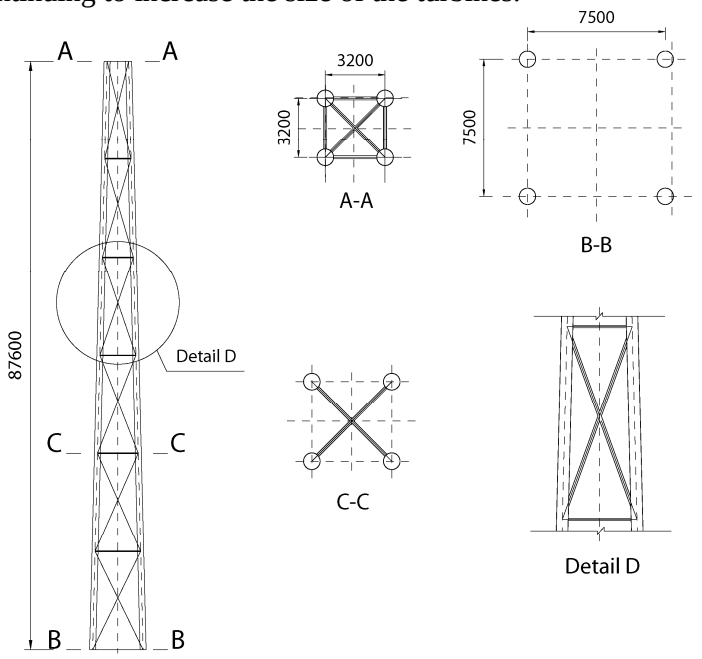

Fig. 5. Layout of a truss tower. Units in millimeters. (Adapted from [23]).

One possible new solution for an offshore turbine would be to use a truss type structure for the entire tower, see Moe et al. [23]. This was to the authors' knowledge never performed before. A preliminary study was made comparing with the NREL 5 MW

Baseline Wind Turbine Model [24] which is based on a tubular tower. Fig. 5 shows the model used for the truss tower. The natural frequencies, static stresses, and buckling were verified and found to be satisfactory. The tower was found to be relatively soft in torsion, which would not be a problem if individual pitching of the blades was performed. This preliminary study showed that the weight of the truss tower was half that of the tubular tower, making the former a promising new solution that should be studied further.

Regarding the foundations for offshore wind farms, solutions that have been used up to now, for existing parks built in waters shallower than 30 m, are of two types: monopile or gravity based foundations. They are illustrated in Fig. 6 as (a) and (b). The choice between these two solutions depends on the type of soil at the base of the turbine. The latter (b) can be installed by drilling and grouting, or by driving [25]. Friction and bearing forces are then used to support the structure. The former (a) makes only use of bearing forces, where a big and heavy concrete or steel caisson is placed on the seabed, supporting the turbine structure. These solutions are limited to shallow waters, as for deeper waters the gravity foundation would become too expensive, and the current technology concerning monopiles is not developed enough [25]. An alternative to these solutions in shallow waters, that is being tested at Fredrikshavn, in Denmark, is the suction caisson (Fig. 6(c)), which is expected to require a simpler construction procedure and to use less material than the gravity foundation [26]. By removing the water from a caisson onto which the turbine is situated, the suction force thus created is used to promote easy installation.

For waters deeper than about 30 m, multiple footing options would have to be used to allow the structure to be stable enough at reasonable costs. They could for example rely on either multiple piles driven into the ground (Fig. 6(d)), or suction piles (Fig. 6(e)). The Beatrice demonstration farm at a 45 m water depth uses the former option.

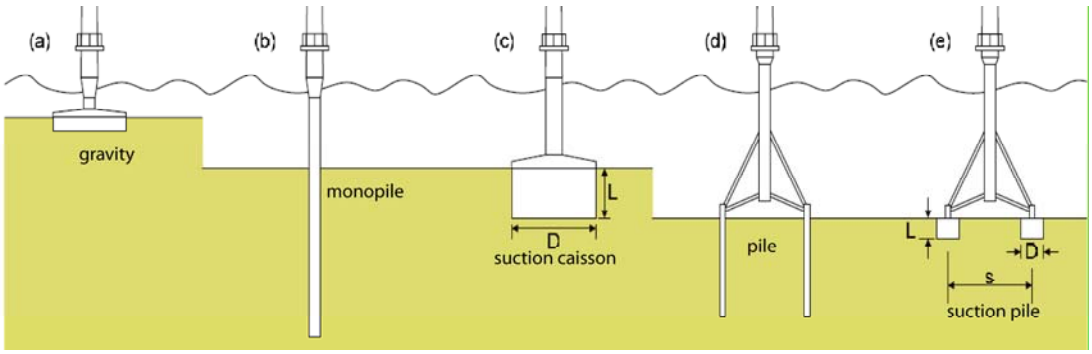

Fig. 6. Options for offshore wind turbine foundations. (Adapted from [25]).

As water depth continues to increase, a certain point is reached for which it would not be economically or technologically feasible to have structures resting directly on the seabed to support the turbine structure. Floating options are being investigated for such cases, for which the load would be carried by the buoyancy force. In this regard, experience developed in the offshore oil and gas industry in countries like Norway, the US and UK could be highly valuable. Three concepts are now being considered for this case, see Fig. 7.

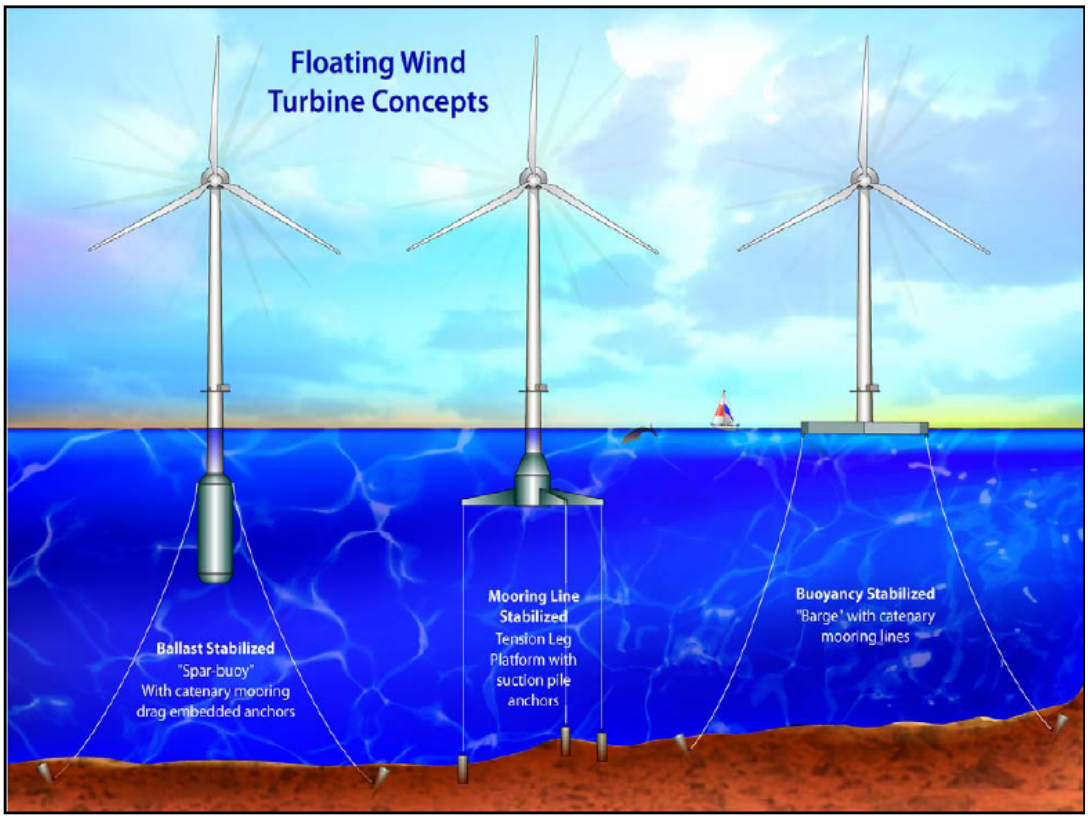

Fig. 7. Floating support platform concepts for offshore wind turbines [27].

The Ballast Stabilized concept is being investigated among others by Norsk Hydro (now StatoilHydro) [28,29]. In this case, ballast is used to get the center of gravity well below the center of buoyancy, providing stability. Catenary mooring lines are used to keep the system in place. Norsk Hydro's concept, called Hywind, consists in the version shown in Fig. 8 of a 5 MW upwind turbine with a 123 m diameter three-bladed rotor lying 81.5 m above the sea line, mounted on a standard tubular tower and moored by three mooring lines. The concept would be used in water depths from 200m to 700m. What makes this concept particularly interesting is that tests on a scaled down turbine ($1/47^{th}$ of the original model) were performed in a 50 x 80 m^2 ocean basin, where the measured responses were compared to results obtained from a simulation code resulting from the coupling of both an aeroelastic and a marine structure dynamic response code [28]. StatoilHydro plans to install a 2.3 MW prototype of this concept by 2009 in the North Sea. The company Oceanwind Technology is also studying a ballast stabilized concept [30], where they suggest that anchors could be shared between the different turbines in a wind park. In their patented concept (Fig. 9), so-called floating units including a wind turbine would be linked to each other and/or to anchors in a certain geometrical pattern by an arrangement of cables, where the turbines would be separated by at least five diameter rotors. The suggested sharing of the anchors between the units would according to this company result in important anchoring cost reductions.

Fig. 8. Norsk Hydro's floating wind turbine concept [31].

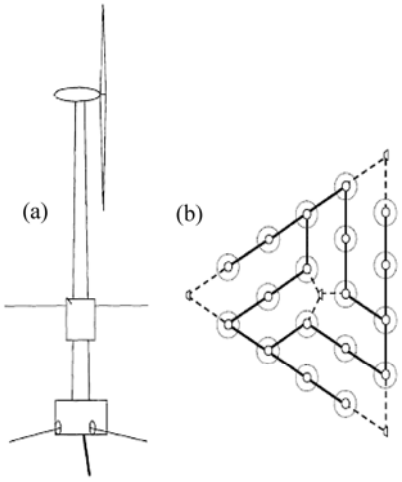

Fig. 9. Oceanwind Technology LLC's concept: (a) floating unit, (b) example of geometrical pattern into which the floating units represented by concentric circles can be arranged. Only four anchors shown by trapezes at the end of the dashed lines are used to keep the arrangement in place. (Adapted from [30]).

NREL, together with MIT, is studying a Tension Leg Platform for a floating wind turbine [32]. The corners of their platform, designed for water depths from 60 m to 200 m and for a 5 MW turbine, would be connected by pretensioned mooring lines anchored to the seabed by suction piles. The pretension in the lines is intended to stabilize the turbine in heave, pitch and roll. Dynamic modelling of this concept in wind and wave conditions has already been made with promising results [32]. A half-scale prototype of this system is hoped to soon be installed in the US [33]. The company Sway [34] is

studying a concept that is a cross somewhere between a ballast stabilized and a mooring line stabilized platform, see Fig. 10. Their proposal is for a 5MW downwind turbine using a streamlined tower to minimize its effect on the rotor. The tower is extended about 100 m under the water surface, and about 2000 tons of ballast are placed at its bottom to stabilize the structure. Anchoring is performed using a single tension leg. The company announced in July 2007 that it had received 150 MNOK [35] to develop and commercialize its technology. The turbine would be installed in water depths from 80 m to 300 m. A full scale prototype is planned for 2010.

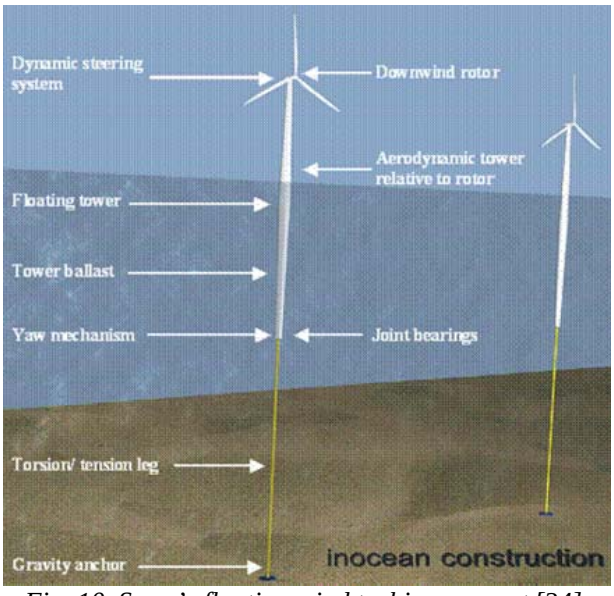

Fig. 10. Sway's floating wind turbine concept [34].

The idea of the Buoyancy Stabilized concept is to have the wind turbine stand on a platform floating near to the surface, and held in place by mooring lines. The lines in this concept have primarily the role of keeping the structure in place. NREL and MIT are also working on such a concept [27,32] to support a 5 MW wind turbine. Modelling of the fully coupled aero-hydro-servo-elastic response of a floating barge supporting a wind turbine at a water depth of 150 m was performed. It was found among other things that this concept would suffer from excessive pitching motions during extreme wave conditions [27]. This is to be expected, since the floating platform has to follow the motions of the waves. Passive control systems were however suggested to try to diminish this motion.

Thus many options are possible, and much research remains to be done to develop a feasible concept that would allow the harvest of enormous amounts of energy from offshore wind blowing above very deep waters.

Concerning transportation of the turbine structures to the offshore sites, what has been done up to now is to transport the components to the site and install them one by one, i.e. the tower modules, nacelle, and blades, using large floating cranes. The rotor can also be mounted onshore [36]. Mounting the components separately offshore takes a lot of time and is costly, floating cranes being very expensive. Costs can also increase if the

installation takes longer than planned due to difficult weather conditions. A new strategy that could be used in the future to reduce costs would be to mount the whole wind turbine as a floater in sheltered waters, tow it to the site, and sink it down in place on preinstalled foundations. The use of cranes could then be avoided, resulting in huge cost savings. Such a procedure is actually proposed by StatoilHydro and Sway for their floating turbine concepts, and also by the inventors of the Oceanwind concept, where the whole floating unit would be floated to its offshore location. However, to our knowledge, such a solution has not yet been developed for bottom-fixed wind turbines.

V. Conclusion

Offshore wind energy has been discussed briefly and has been found to have some advantages over its onshore counterpart. However, many challenges remain regarding this rather new technology. Several offshore wind parks have been developed in Europe, but the technology is still at an early stage. The conditions in North-America are rather different from those in the European waters currently used for wind parks. Therefore solutions that are being developed and implemented in Europe will probably not be optimal in North America, where no offshore parks are yet installed, but where the potential for this clean energy source is enormous. New technologies will have to be developed in order for large scale offshore wind parks to be installed in North America, as well as in European sites differing from those that have been used up to now. Research is also needed to create wind turbines more adapted to offshore conditions, and to develop feasible and cheap foundations and installation procedures. Successful floating turbine concepts would in the future also make it possible to harvest huge amounts of clean energy far out in the oceans. Offshore wind energy is indeed a very promising field. Let us conclude by citing a recent paper regarding offshore wind energy [37], which provides solid ground to continue developing this clean and renewable energy source: "*Wildlife impacts (and other externalities) that result from wind generated electrical power, however, should not be viewed in isolation, but rather need to be considered relative to the wildlife impacts and other environmental consequences from other forms of energy production […] In sum, a complete and balanced evaluation of offshore wind energy must consider not only the wildlife impacts of wind development, but the wildlife impacts should the potential for offshore wind energy not be realized, that is, continued growth of fossile fuel production and its associated environmental and wildlife degradation.*"

REFERENCES

[1] European Wind Energy Association. EWEA's response to the European Commission's Green Paper "Towards a future Maritime Policy for the Union: A European vision for the oceans and seas". Brussels, June 2007.

[2] *Offshore Wind Energy Europe*. (2007, June 28). Retrieved September 14, 2007, from www.offshorewindenergy.org

[3] Chair of the European Policy workshop on Offshore Wind Power Development. Berlin Declaration, Conclusions of the Chair. Berlin, February 2007.

[4] Danish Energy Agency. Offshore Wind Farms and the Environment, Danish Experiences from Horns Rev and Nysted. Copenhagen, November 2006.

[5] *British Wind Energy Association*. (2003). Retrieved September 14, 2007, from http://www.bwea.com/images/media/HornsRev-Denmark.jpg

[6] Global Wind Energy Council. Global Wind 2006 Report. Brussels, 2007.

[7] *Beatrice Wind Farm Development Project*. (2007). Retrieved September 14, 2007, from http://www.beatricewind.co.uk

[8] Greenpeace, Global Wind Energy Council. Global Wind Energy Outlook 2006. Brussels, September 2006.

[9] Hersleth P. 1000 MW i 2012. Oslo, June 2007.

[10] Burgermeister J. (2007, August 3). Spain to Allow Offshore Wind Farms. *Renewable Energy World.com*. Retrieved September 14, 2007, from http://www.renewableenergyaccess.com/

[11] U.S. Department of the Interior. Technology White Paper on Wind Energy Potential on the U.S. Outer Continental Shelf. United States, May 2006

[12] Butterfield S, Ram B, Musial W. US Offshore Technology Overview. Boulder, Colorado, June 2007.

[13] *Canadian Wind Energy Atlas*. (2006). Retrieved September 14, 2007, from http://www.windatlas.ca/

[14] *Offshore Wind Energy Europe*. (2007). Retrieved September 14, 2007, from www.offshorewindenergy.org

[15] *Cape Wind*^{TM}. (2007). Retrieved September 14, 2007, from www.capewind.org

[16] *BluewaterWind*. (2007). Retrieved September 14, 2007, from http://www.bluewaterwind.com/delaware.htm

[17] *LIPA's Offshore Wind Park*. (2006). Retrieved September 14, 2007, from http://www.lipower.org/cei/offshore.history.html

[18] Shannon K. (2005, October 25). Texas sells lease for a major wind farm. *The Boston Globe*. Retrieved September 14, 2007, from www.boston.com/news/

[19] Naikun Wind Development Inc. (2007). Retrieved September 14, 2007, from http://www.naikun.ca/

[20] International Energy Agency. Offshore Wind Experiences. Paris, 2005.

[21] Malcolm DJ, Hansen AJ. WindPACT Turbine Rotor Design Study. National Renewable Energy Laboratory. *NREL/SR-500-32495*, Golden, CO, August 2002.

[22] Moe G. What is the Optimum Size of a Wind Turbine? *Proc. of the 26th International OMAE Conference*, San Diego CA, 2007.

[23] Moe G, Niedzwecki JM, Long H, Lubbad R, Breton SP. Technology for offshore wind turbines. *Proceedings of the Fourth International Conference on Fluid Structure Interaction*, The New Forest, UK, 2007.

[24] Jonkman J, Butterfield S, Musial W, Scott G. Definition of a 5-MW Reference Wind Turbine for Offshore System Development. *NREL/TP-500-38060*, National Renewable Energy Laboratory, Golden, CO, 2007.

[25] Byrne BW, Houlsby GT. Assessing novel foundation options for offshore wind turbines. *Proceedings of the World Maritime Technology Conference*, London, March 2006.

[26] Danish Energy Agency. Offshore Wind Power, Danish Experiences and Solutions. Copenhagen, October 2005.

[27] Jonkman JM, Buhl ML Jr. Loads Analysis of a Floating Offshore Wind Turbine Using Fully Coupled Simulation. *Proceedings of WindPower 2007 Conference and Exhibition*, Los Angeles, California, 2007.

[28] Skaare B, Hanson TD, Nielsen FG. Importance of Control Strategies on Fatigue Life of Floating Wind Turbines, *Proceedings of OMAE 2007 26th International Conference on Offshore Mechanics and Arctic Engineering*, June 2007, San Diego, CA.

[29] Nielsen FG, Hanson TD, Skaare B. Integrated Dynamic Analysis of Floating Offshore Wind Turbines. *Proceedings of OMAE 2006 25th International Conference on Offshore Mechanics and Arctic Engineering*, June 2006, Hamburg, Germany.

[30] Yamamoto S, Colburn WE Jr. Power Generation Assemblies. International Patent, Publication Number W0 2005/040604 A2, May 2005.

[31] *Norsk Hydro ASA*. (2007). Retrieved September 15, 2007, from www.hydro.no

[32] Wayman EN, Sclavounos PD, Butterfield S, Jonkman J, Musial W. Coupled Dynamic Modeling of Floating Wind Turbine Systems. *Proceedings of the Offshore Technology Conference*, Texas, May 2006.

[33] NAW staff. (2006, September 13). MIT, NREL Study Floating Turbine. *North American Wind Power*. Retrieved September 15, 2007, from www.northamericanwindpower.com/

[34] *Sway*. (2007). Retrieved September 15, 2007, from http://www.sway.no/

[35] Borgen E, Steine AO, Aamodt A, Gravdal A, Røst S. (2007, July 11). Sway raises NOK 150 million to realize deepwater wind turbines. *Press release*. Retrieved September 15, 2007, from http://www.sway.no/

[36] *Offshore Center Danmark*. (2007). Retrieved September 15, 2007, from http://www.offshorecenter.dk/teknologi-vindmoeller.asp

[37] Firestone J, Butterfield S, Coakley C, Jarvis C, Clarke J. Offshore Wind Power on the Horizon: A New Energy Frontier for Oceans, People and Wildlife. *The Coastal Society Proceedings and Final Program*, Tampa Bay, Fl, May 2006.

6. DISCUSSION AND CONCLUSIONS

Let us first look at the principal wind turbine aerodynamic load prediction methods, which will lead to a justification of the method that was used for the work performed on the stall delay phenomenon. Different issues raised by the articles presented will then be reexamined, before conclusions are finally made on the work performed.

6.1. Principal prediction methods, and justification of the method used

6.1.1. Principal prediction methods

a) Blade Element Momentum Method

The Blade Element Momentum (BEM) method, originally developed by Glauert[33] is the most widely used simulation method today for the calculation of loads and design of wind turbines. It combines the concept of the actuator disc with a blade element analysis. The actuator disc is a permeable surface modelling the rotor as being formed of an infinite number of blades, positioned normal to the incoming flow, and through which the flow can pass while applying forces. It is developed by considering the conservation of mass, momentum and energy for the flow passing through it[3]. Dividing it in independent annular elements inside which momentum balance and energy conservation are applied results in a system of equations for the thrust and torque on the annular elements, that are dependant on the relative velocity seen by the blade element, and therefore, on the induced velocities at the blade. An iteration process is performed, which allows to compute these induced velocities, and thereby, the angle of attack on the elements. This finally allows loads on the individual elements to be found. Airfoil data in the form of lift and drag coefficients as a function of angle of attack are used in this process, as well as the geometry of the blades, which is necessary to the

calculation of the angle of attack locally on the blade. While the BEM method is easy to implement and widely used, it suffers from some limitations. For example, the modelling as an infinite number of blades, resulting in axial symmetry, renders this method dependant on the use of tip loss models. It also considers the induced velocity on the actuator disc to be equal to half the induced velocity in the far wake[3], which is not exact, and assumes independent elements along the blade, neglecting the presence of radial flow. Moreover, it is not inherently built to handle unsteady inflow, as it is fundamentally based on the use of a disc positioned normal to the incoming flow.

b) Actuator line and actuator disc methods

To remedy some of the limits of the BEM method, new models have been recently developed, also based on the actuator disc concept. In the generalized actuator disc method[34,35,36,37], this concept is used to calculate volume forces on the disc, which are found by combining a blade element approach with the use of airfoil data. However, in this case, kinematics of the flow is governed by the use of the axisymmetric Euler or Navier-Stokes equations. In fact, the main improvement over the BEM method is said to consist in the replacement of the annular independence of the blade elements intrinsic to this method by a full set of Euler or Navier-Stokes equations[38]. The presence of the rotor is actually replaced by the above-mentioned volume forces that are incorporated into the Euler or Navier-Stokes analysis as source terms[34]. The actuator disc is then in this case used as a model that makes it possible to put discontinuities into the flow equations. A solution is searched from an iterative process considering the mutual interaction between the blade forces and the flow field. As a disc is used in this process, axial symmetry is supposed, so that the resulting loading is not dependant on the azimuth position. This requires as in the BEM method the use of a tip loss model to

account for a finite number of blades[35]. Recently, an improved version of the actuator disc model was developed by Sørensen and Shen, called actuator line[38], that does not contain this axisymmetric assumption. In this model, the effect of each rotating blade is rather directly modelled by a line on which body forces, found once again from the use of airfoil data, are distributed.

c) CFD and hybrid methods

Another way to proceed is to separate the space around the wind turbine in a grid composed of many cells inside which the partial differential equations describing the flow, i.e. the Navier-Stokes equations, are solved. This depicts a complete image of the flow environment with a resolution corresponding to the resolution used for the grid. This procedure is known as Computational Fluid Dynamics (CFD), and does not depend on the use of airfoil data. Its capacity to provide detailed information about the flow on a rotating blade, particularly within the boundary layer, makes it very powerful to study among other things its separation. As such, it would be useful to study the stall delay phenomenon in a next step, and it was already used in that sense by some authors[29,39,40]. This method however suffers from very high computational costs, due to the very large number of calculations to be performed. For this reason, models have been developed that combine the use of the CFD technology with the vortex wake methods that will be discussed shortly. In such cases, CFD is used in a grid surrounding the blades to model the important phenomena occurring in this area, avoiding by the way the use of airfoil data, while a vortex wake method models the wake behind the blades. Schmitz and Chattot[41], as well as Benjanirat and Sankar[42], are examples of authors having developed such methods. While promising results were said to have been obtained by Schmitz and Chattot using this technique, Benjanirat and Sankar found that the higher computational

costs involved from using CFD everywhere in space were worth investing in view of the better correlation obtained with experiment.

d) Vortex wake methods

In vortex wake methods, the blades are replaced by either a lifting line or a lifting surface, defining the two categories of such methods. The wake formed behind the blades, resulting from spatial or temporal changes of circulation along the blades, is modelled as vortex elements or particles which are kept track of as they move downstream. This is referred to as a Lagrangian manner[43] of modelling the flow, while in CFD methods an Eulerian representation is often used, where space is divided into fixed cells inside which the Navier-Stokes equations are solved. The vortex elements or particles induce velocities everywhere in space, in the same way as an electric current induces a magnetic field. The Biot-Savart law is actually used in both these cases to find the resulting induction. Let us now discuss the two types of vortex wake methods, namely the lifting surface and lifting line methods.

-Lifting surface methods

The lifting surface methods include the vortex lattice and vortex particle methods. Bertin and Smith[44] explain the idea behind the vortex lattice method for a non-rotating wing when only the velocities induced by the wake on the blade are considered, neglecting self-induced velocities in the wake. The key is the use of horseshoe vortices, which have a constant strength along their length. The blade is separated in spanwise elements, which are usually themselves divided into panels. To each panel is associated a horseshoe vortex and a control point. One begins by considering a control point on a given panel, where the different horseshoe vortices induce a velocity, calculated from the Biot-Savart law using the simple expression for the velocity induced by a semi-

infinite line vortex. A flow tangency condition, called kinematic boundary condition, is used, stating that the total velocity at the control point has to be parallel to the surface. This is the key boundary condition to this method, which apropos neglects the effects of viscosity and thickness of the blade in its basic formulation. Using this condition at every control point results in of a system of equations which is to be solved for the circulation related to every horseshoe vortex. This basic method has been extended to the more complex case of rotating blades and is used by many authors today, with a varying degree of consideration of the self induction of the wake. When the blades are rotating, the vortices become helicoidal, and have to be separated into elements to compute the velocity they induce on the blades, but possibly also on the other elements in the wake. The velocities induced by the horseshoe vortices can no longer be found using the expression for the induction from a semi-infinite line vortex. In fact, the vortices being helicoidal, the velocities induced at a certain control point now depend on the position of each vortex element. The Biot-Savart law is used to calculate the velocity induced by a straight line vortex segment, and, using the tangential flow boundary condition, a set of simultaneous linear equations is obtained. The solution to this set of equations gives the vortex strengths on the rotor and in the wake. Among others, Simoes and Graham[45,46,47], Rosen et al.[48], and Bareiss and Wagner[49,50], have used the vortex lattice method, which they subjected to the same approximation, namely to model self-induced effects only in the part of the wake located nearest to the blades, called the near wake. Pesmajoglou and Graham[51] also developed such a method, where however they did not restrict self-induced effects to the near wake.

In the vortex particle method, the vorticity in the wake is represented as a set of vortex carrying particles, while the blades are modelled as a lifting surface where

thickness effects are neglected. The vorticity transport equations, the Biot-Savart law as well as the flow tangency condition are used to govern the development of the wake. This method was applied in wind turbine simulations by for example Zervos et al.[52] and Voutsinas et al.[53].

-Lifting line methods

In the lifting line method, the blades are replaced by a line of bound vorticity which can vary in strength due to the introduction of trailing vorticity carrying radial differences in circulation. Changes in bound vorticity with time result in vorticity being shed from the blades. The value of the bound vorticity Γ is determined from applying the Kutta-Joukowsky law[21], which relates this vorticity to the lift L, the effective incoming wind velocity V_{rel} seen by the blade, and air the density ρ:

$$L = \rho V_{rel} \Gamma \tag{6}$$

This law is the generalization of the effect from the bound vorticity inducing velocities on both sides of a lifting body that result in a pressure jump at the source of the lift force (Section 4.3.2). In the present 3D flow case, the free stream velocity used in the 2D formulation of this law is replaced by the effective velocity V_{rel} which includes the induction effects from the wake behind the blades. The lift is determined from airfoil data tables where it is given as a function of the angle of attack. Both the angle of attack and V_{rel} depend on the velocity induced on the blade by the vortex elements in the wake, which is the unknown here. Induction at the blades and everywhere in the wake is found from applying the Biot-Savard law at each vortex element. Vortex elements in the wake are usually modelled by linking two wake points together by a straight line, wake points starting from the blades and travelling downstream at each time step with the free stream velocity plus the induction created by the other vortex elements. In practice, the

vortex elements can be given different levels of freedom, considering for example their induction only in some parts of the wake, or restricting the development of the wake itself in different ways. When no such restrictions are used, the method is referred to as "free wake". Free wake methods are computationally very demanding, because a very high number of calculations are required at each time step to find the induction of every vortex element on every other element.

In the free wake method, stability problems may occur if two given vortex elements come too close to each other, resulting in too large induced velocities. This can be solved to a certain extent by the modelling of a viscous core size inside which the induced velocity decreases from its value at the radius of the core[54,55]. In this method, as the vortex elements are completely free, points at the boundary of a given element may move relative to each other, resulting in stretching of the elements. Following Helmoltz's third law, the net strength of any vortex element must remain constant, which requires the product of the vorticity and the cross-sectional area of the element to also remain constant[56]. When the vortex element is stretched, its vortex core size is decreased, which leads to an increase in its vorticity. Vortex diffusion also has an effect on the size of the vortex core, which increases as the vortex elements age[54], or move downstream. These two effects on the vortex core size are known to be difficult to distinguish[56], and they make the computations even more difficult. Convergence problems may happen if wake points at the boundary of given vortex elements begin to move in completely different directions, resulting in non physical elements. Convergence problems may also follow from numerical error instabilities growing with time[57], as round-off or truncation errors. Such instabilities resulting from the free wake

modelling have been known to be difficult to distinguish from actual physical instabilities of rotor wakes[7].

Free wake methods have been developed for helicopter wakes by for example Clark and Leiper[58], and later by Leishman's group at the University of Maryland[56,59,60], who also studied many aspects regarding stability of the physical wake[61,62,63] and of the simulation method itself[57]. Leishman's group also developed a similar method for wind turbines[7,64], as well as Gohard, who was the first to apply it to wind turbines[65].

Difficulties mentioned above regarding lifting line modelling using a completely free wake explain why many models have been developed that restrict the development of the wake in some manner, resulting in different simplifications. For example, Afjeh and Keith[66] developed a model called the Simplified Free Wake Model (SFWM), where the most important approximation consists in the use of a prescribed near wake. Miller[67,68] introduced a prediction method called the fast free wake method (FFWM), where wake displacements are dictated by average velocities determined from using the velocities below the blades. In the lifting line model that Dumitrescu and Cardos formulated[69], vortex elements are restrained to a prescribed path, while in the rigid wake model developed by Kotb and Abdel Haq[70], wake displacements are determined using only the velocities at the blade from which the vortex elements were formed. Prof. Coton's aerodynamics research group at the University of Glasgow developed a lifting line model using a prescribed wake[71], whose use in the present work is now further discussed.

6.1.2. Justification of the method used

The lifting line prescribed wake model that was used in this work is well described in the two first articles above. This model had been used in numerous studies

before by Prof. Coton's group[5,71,72,73,74,75] and led to satisfactory results. It was also used in the blind comparison exercise following NREL's wind tunnel tests[10]. It offers a physical representation of reality, and it was seen as a good compromise for the study that was to be performed on stall delay models. It is based on the use of airfoil data, as the other lifting line codes mentioned above, as opposed to lifting surface and CFD based codes, so that it makes it possible to study the corrections performed by stall delay models on these data. This method is also less computationally demanding than CFD models, and renders the tracking of the vortex elements in the wake possible, which cannot be achieved with BEM methods. This tracking, among other things, allows one to study the effects from the tip vortex. Moreover, modelling of the wake with this method is feasible without the convergence problems that can follow from the use of a completely free wake. Through the use of this modelling code, a collaboration with Prof. Coton's research group was realized. This group, that has a long experience in helicopter as well as wind turbine aerodynamics, allowed us to work with their code and modify it for our purposes. It was then possible to understand every step of its operation and of the vortex wake modelling, what would not be the case if a black box type of code were used. In summary, this method was well suited for the study performed here, and this is why it was chosen.

6.2. Reexamination of Issues Raised by the Articles

The work accomplished on investigating the stall delay phenomenon and models intended to correct for its effects concluded that none of the models studied represented the flow physics correctly, and that this was ultimately responsible for their lack of generality. The separation of the boundary layer from a surface is already a complex phenomenon, and rotation produces a far more complicated situation, as elaborated on

in section 4.4, and discussed in the articles above. This makes it difficult to understand the basic flow mechanisms related to stall delay, and even more so to represent them in a correction model. The effects on the attached and separated boundary layers from the Coriolis and centrifugal forces, and from the spanwise pressure gradient, have to be represented in a model with a weight corresponding to their relative importance. This is a difficult task as these effects are not yet fully understood, and as there exists no clear consensus on their relative importance[76]. The results obtained clearly show that further work is needed in exploring the different mechanisms involved in the boundary layer behavior on a rotating blade.

One way to better understand the mechanisms involved is to carefully scrutinize and compare pressure measurements performed on a rotating and a non rotating blade. By comparing near stall behaviour for the two cases, valuable information about the effects of rotation on stall can be found. Great efforts along these lines have recently been performed by Schreck and Robinson using the NREL wind tunnel data. For example, they visualized surface pressure topologies and could thereby learn about the relationship between chordwise and spanwise pressure gradients, and their implication in the separation of the boundary layer[77]. Among other things, these pressure distributions were found to clearly indicate that the increase of the lift force associated with a rotational condition, or rotational augmentation, was intimately related to the development of spanwise pressure gradients. Schreck and Robinson also related the standard deviation of the measured surface pressure to the boundary layer separation[76]. Further work by Schreck et al.[4] combined the latter experimental analysis with CFD computations that could provide more detailed information about the boundary layer than available from measurements, as well as inform about above-surface flow field

structures. These are important examples of work using the NREL wind tunnel data that allowed light to be shed on the mechanisms involved in the stall delay phenomenon. Further tackling of the NREL wind tunnel test data along the lines presented here could help push the understanding further by revealing more about the structures and interactions responsible for the rotational augmentation, as suggested by Schreck and Robinson[77].

Recent tests performed in the biggest wind tunnel in Europe in 2006 could also be used to further study the phenomenon of stall delay[78]. These tests were referred to as MEXICO, for Model Rotor Experiments under Controlled Conditions. The experiments were performed on a three-bladed rotor of 4.5 m in diameter, in a wind tunnel of dimensions 9.5 x 9.5 m^2. Pressure was measured at in total five different radial positions shared between the three blades. Two blades had instrumented sections at two different radial positions, while the third blade had pressure sensors at one position only. This can inform, as in the NREL experiments, about the behavior of the boundary layer on the rotating blades. Tests that were performed on parked blades make it possible to compare the rotating and non rotating conditions. Root bending moments were also measured at the root of the three blades. A notable difference from the NREL experiments is that Particle Image Velocimetry (PIV) measurements were performed. Flow visualisation was performed in the NREL wind tunnel tests with the help of smoke generators located at the blade tip[11], but PIV goes a step further as it allows the determination of the 3D flow field quantitatively. This makes it possible to study the wake behind the turbine, which can inform about the boundary layer separating from the blades and being transported downstream. Special attention was also given to the tip vortex in these PIV measurements. This can help one understand the loss effects it causes in the tip region,

and better model them. These effects were shown above to be central to accurate load predictions. CFD simulations were suggested above to further study the effects from the tip vortex, but these measurements could also be of great use.

CFD computations could also eventually be used to model the effect of the boundary layer transition. Fig. 11 shows as an example the Reynolds number found on the NREL blade as a function of incoming wind speed for the five spanwise positions studied. Reynolds numbers above 5 x 10^5 correspond to a turbulent boundary layer on an airfoil[79]. Reynolds number above this value are observed everywhere on the blade in Fig. 11, which means that transition from a laminar to a turbulent boundary layer has to happen on this blade. As mentioned in the second article presented above, the transition of the boundary layer state from laminar to turbulent can have a significant impact on the separation process that should be studied further. Finally, using the knowledge from some of the above-mentioned approaches, new correction models could eventually be developed.

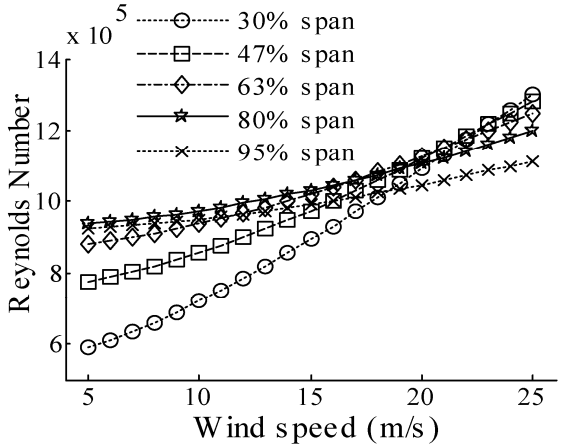

Figure 11. Spanwise variation of the Reynolds number on the NREL blade

The study of root bending moment estimates performed in the third article suggested a significant systematic error in the NREL measurement of the root flap bending moment in the upwind configuration. This has important implications, because

these measurement data are used to verify the accuracy of prediction models. Prediction models, in turn, are used in the design of wind turbines. The more uncertain the predictions are found to be, the more conservative the design of wind turbines will have to be, resulting ultimately in higher costs. It was therefore considered important in this case to determine if the difference in mean value observed for the root flap bending moment resulted from the measurements or from the predictions. As seen above, our analysis pointed towards a reliable aerodynamic estimate, which suggested problems with the measurement of the root flap bending moment in the upwind configuration. The data from the MEXICO wind tunnel tests could be used as a tool to validate the model predictions of the root flap bending moment. It would be a great opportunity to predict the root flap bending moment on a different rotor design, and see if a systematic difference at low wind speed is still observed in the upwind configuration. A prediction from the same simulation model that would not result in such a difference for this distinct rotor design would be another argument pointing towards a systematic error in the measurement of the root flap bending moment on the NREL rotor in the upwind configuration. Measured torque forces could also be used to calculate the power produced and compare it with the direct measurement, informing once again about possible problems with the measurement of tangential forces at high wind speeds.

The NREL wind tunnel test data were found to be very useful in studying dynamic effects on wind turbine blades, even though the latter were known to be quite rigid. Dynamic effects on wind turbine blades have important implications on a wind turbine. It is so on a short time basis, where for example too large oscillations of the blades can damage the structure, and these effects are also crucial on a long term basis, where wind turbines that are designed to last at least 20 years will experience about 10^9

revolutions in their lifetime[80]. This means that each blade of a downwind turbine will suffer an impulsive load due to the tower shadow about 10^9 times. Let us note that many other causes for dynamic effects also exist, like turbulence in the incoming flow, yaw error, and pitch regulation. Such effects have to be quantified in order for a reliable fatigue analysis to be performed. This is especially relevant for offshore applications where downwind turbines are seen as a valuable alternative as discussed above, and where the suggested use of softer blades would result in significant dynamic motions, but not necessarily larger stresses. The use of a truss tower also advanced above as a possible alternative for offshore turbines is expected to result in less pronounced shadow effects, which would be interesting to characterize and compare with the effects from a cylindrical tower. The wake resulting from a truss tower is very different and its effects on the blades are expected to differ too. As no experimental data is known to be available for such a tower, modeling would constitute a first step.

The model built to calculate aerodynamic estimates for the root bending moments was seen to reproduce quite well most of the dynamic effects observed in the measurements, as well as predict the mean value of the moment in a satisfactory way. This is an indication of the reliability of this model, whose use could then be extended to predictions concerning other turbines. However, in the case of larger turbines, other effects would come into play and have to be considered. It was discussed above that the contribution to the bending moments from centrifugal forces resulting from the elastic deformations of the blades was not significant in the case of the NREL blade. This effect would have to be considered on larger turbines where it would contribute significantly to the total moment[81]. The method would also have to be combined with an aerodynamic simulation code that would predict the aerodynamic loads to which the

blades are exposed, in cases where measured aerodynamic forces are not available. Aeroelasticity would become an important issue, where the oscillations experienced by the blades would change the relative wind velocity that they see, modifying the aerodynamic loads relative to the ones experiences by a rigid blade. Coupling would then have to be made between a structural dynamics simulation code as the one presented above and a code intended to predict the aerodynamic loads. Extensive work has already been performed on this subject, see as a few recent examples the work from Madsen et al.[82], Hansen[83], and Riziotis et al.[84], as well as review article by Hansen et al.[6] Let us note that oscillations of other parts of the wind turbine, like the tower and nacelle, may also play an important role in the aeroelastic behavior of the turbine[85]. Aeroelasticity of wind turbines still is the object of much investigation, as it is of crucial importance for today's modern large wind turbines whose more flexible blades suffer from significant vibrations.

The research performed on offshore wind energy and presented above allowed one to get an overview of the status and plans for this rather new technology in Europe and North America, and of new solutions that could be more adapted to this technology. Things are evolving very quickly in this field. Since the redaction of the journal article treating offshore wind energy, that was performed at the end of 2007, events worth noting have taken place. For example, the United Nations Climate Change Conference held in Bali in December 2007 led to important commitments regarding offshore wind energy. Germany appeared as a leader when it revealed its plans for reducing its greenhouse gas emissions by 40% by 2020[86]. To reach this target, the use of renewable and clean energy sources was brought forward, with offshore wind energy at the top of the list. UK also in December 2007 announced[87] enormous offshore development

projects. Plans are to build 25 GW of new offshore wind turbines by 2020, adding to the 8 GW that are to be produced by projects already approved or under construction. Norway also announced recently[88], in January 2008, that it will invest large amounts of money (e.g., 150 MNOK in 2009) into the development of renewable energy technologies offshore, of which wind energy will get the Lion's share. The public funds for research on renewable energy sources have been announced to become at least equivalent to the public investments within oil research by 2010. Public acceptance has been an important issue in the development of wind energy in Norway, and it is expected that the deployment of offshore turbines will be easier than onshore. The status of offshore wind technology is evolving very fast in North America, even though no park is yet in operation. As a few examples, a major win has recently been made for the Cape Wind project which has been given preliminary environmental approval by the US Federal Minerals Management Service which is known to be the key federal unit to decide if the project will go forward[89]. Wind Energy Systems Technologies LLC has recently been allowed the first four bid leases for offshore wind energy development in US history, and now plans to build at least 250 MW to 300 MW per lease[90], which is far more than the total 150 MW originally planned. Projects are also planned to soon be developed on the Canadian side of the Great Lakes, after a moratorium on the development of offshore wind farms in the Great Lakes, that had been imposed in 2006 to study the environmental impacts of such projects, has recently been lifted[91]. In this regard, let us mention that a study performed by Helimax Energy Inc. has evaluated the potential for offshore power to 47 000 MW in the Great Lakes[92].

Colossal developments of offshore wind energy are then expected to be seen both in Europe and North America in the coming years. As regards the development of

new technologies that would be more adapted to offshore technologies, we will have to see if upcoming projects will favor them over the solutions that have been used up to now, which are more adapted to onshore conditions. Chances are that this will happen, as much is to be gained in this regard, and as the offshore market is now beginning to drive the research and development in the wind energy field[1].

6.3 Conclusions

The work presented in this thesis allowed to study different aspects of the wind energy field that were all related, as discussed above. Steps were made in the understanding of rotational effects affecting the flow on a wind turbine, as well as of dynamic effects experienced by the blades. Ideas on future work to be performed have also been put forward, because even though great advancements in wind turbine technology have happened in the past 20 years or so, much remains to be done in understanding basic phenomena that will ultimately lead to more optimal designs and reduced costs.

The future looks very bright for wind energy, which is establishing itself as a full-fledged and sustainable industry. More and more countries are investing in wind energy every year, and this shows no sign of stopping anytime soon. Attention in the next years will be focused offshore where colossal developments are expected. This technology being quite young, new countries that have not yet participated actively to the onshore development of wind energy may now be able to play a significant role. For example, Norway, which has a long experience with offshore oil, might soon enter this field, considering the recent commitments it made towards developing renewable energy sources offshore. This is even more plausible if it succeeds in developing an operational floating turbine, on which it already has put great efforts. North America,

which has been late in its onshore development relative to Europe, may also soon become an important player.

Let us finally hope that wind energy will keep evolving as quickly and sustainably as in the last 20 years, helped by research advancements that will make it ever more cost-effective and attractive. It should then be able to supply the world with an ever greater amount of clean energy and thereby help reduce CO_2 emissions, limiting climate change and leaving a brighter future for the generations to come.

ACKNOWLEDGMENTS

I am grateful to many people for making this great adventure possible. First of all, I would like to express my sincere gratitude to my supervisor Prof. Geir Moe for his constant help throughout my PhD, and for having believed in me from the start. I wish to thank him for the freedom he gave me in my research project and in the ways to achieve it, for his support, generosity, and great understanding. I would also like to thank Prof. Frank Coton from the University of Glasgow, who gave us access to the vortex wake simulation code used in this study, who was always willing to help me, and very patient in rigorously answering my questions that often took the form of very long e-mails. Thanks also to Dr. Hugh Currin from the Oregon Institute of Technology for his help with the code, and to Philippe Beaucage from Institut national de la recherche scientifique in Varennes, Canada, for great discussions regarding wind energy. I am also very grateful to the Fluid Mechanics group at the Technical University of Denmark, for having welcomed me for a three month research stay in the spring of 2006. Thanks to my colleagues in the basement, for help, great discussions and coffee pauses, and many thanks to Haiyan Long for her patience and generous help concerning the paper we collaborated on. I also want to thank all my friends in Norway for making my stay here nice. Special thanks to Mathieu and Martin for their support.

Thanks to the Fonds Québécois de la Recherche sur la Nature et les Technologies, the UNIFOR Foundation, the Norwegian Research Council, as well as the Center for Renewable Energy at NTNU for financial support.

Finalement, j'offre mes sincères remerciements à ma famille pour m'avoir soutenu dans cette aventure, et à mes amis, avec lesquels j'ai pu partager mes expériences de travail et de vie. À tous, un énorme merci!

REFERENCES

[1] EWEA. "The facts", CD distributed at the EWEC 2004 conference, London 2004.

[2] Global Wind Energy Council. (2007, February 15). Continuing boom in wind energy – 20 GW of new capacity in 2007. *Global Wind Energy Council News*. Retrieved March 9, 2008, from www.gwec.net

[3] Hansen MOL. *Aerodynamics of Wind Turbines*. James and James: London, UK, 2000; Chap. 6.

[4] Schreck SJ, Sørensen NN, Robinson, MC. Aerodynamic Structures and Processes in Rotationally Augmented Flow Fields. *Wind Energy* 2007; **10**: 159-178. DOI: 10.1002/we.214.

[5] Coton FN, Wang T, Galbraith RAMcD. An Examination of Key Aerodynamic Modelling Issues Raised by the NREL Blind Comparison. *Wind Energy* 2002; **5**: 199-212. DOI: 10.1002/we.58.

[6] Hansen MOL, Sørensen JN, Voutsinas S, Sørensen N, Madsen Haa. State of the art in wind turbine aerodynamics and aeroelasticity. *Progress in Aerospace Sciences* 2006; **42:** 285-330.

[7] Leishman JG. Challenges in Modelling the Unsteady Aerodynamics of Wind Turbines. *Wind Energy* 2002; **5**: 85-132. DOI: 10.1002/we.62.

[8] Snel H. Review of Aerodynamics for Wind Turbines. *Wind Energy* 2003; **6**: 203-211. DOI: 10.1002/we.97.

[9] Snel H. Review of the Present Status of Rotor Aerodynamics. *Wind Energy* 1998; **1**: 46-48.

[10] Simms D, Schreck S, Hand M, Fingersh LJ. NREL Unsteady Aerodynamics Experiment in the NASA-Ames Wind Tunnel: A Comparison of Predictions to Measurements. *NREL/TP–500-29494*, National Renewable Energy Laboratory, Golden, CO, 2001.

[11] Hand MM, Simms DA, Fingersh LJ, Jager DW, Cotrell JR, Schreck S, Larwood SM. Unsteady Aerodynamics Experiment Phase VI: Wind Tunnel Test Configurations and Available Data Campaigns. *NREL/TP–500-29955*, National Renewable Energy Laboratory, Golden, CO, 2001.

[12] Moe G, Breton, SP, Schreck S. Assessment of motions and forces in the NREL NASA Ames wind tunnel tests. *2007 European Wind Energy Conference Proceedings*, Milan, Italy, 2007.

[13] Schreck S. The NREL Full-Scale Wind Tunnel Experiment, Introduction to the Special Issue. *Wind Energy* 2002; **5**: 77–84. DOI: 10.1002/we.72.

[14] Schepers JG, Brand AJ, Bruining A, Graham JMR, Hand MM, Infield DG, Madsen HA, Paynter RJH, Simms DA. Final report of IEA Annex XIV : Field Rotor Aerodynamics. *ECN-C--97-027*, Netherlands Energy Research Foundation, Netherlands, 1997.

[15] White FM. *Fluid Mechanics, fourth edition*. McGraw-Hill: New York, 2001; Chap. 7.

[16] Schlichting H, Gersten H. *Boundary Layer Theory*. Springer: Berlin, 2000; Chap. 2.

[17] Hansen MOL. *Aerodynamics of Wind Turbines*. James and James: London, UK, 2000; Chap. 3.

[18] Schlichting H. Boundary Layer Theory. McGraw-Hill: New York, 1979; Chap. 1.

[19] Corten GP. Flow Separation on Wind Turbine Blades. *PhD Thesis*, University of Utrecht, Netherlands, 2001.

[20] Newman JN. Marine Hydrodynamics. MIT Press: Cambridge, MA, 1977; 159-206.

[21] White FM. *Fluid Mechanics, fourth edition*. McGraw-Hill: New York, 2001, Chap. 8.

[22] Abbott IH, von Doenhoff AE. Theory of Wing Sections. Dover Publications: New York, 1959; Chap. 1.

[23] Schlichting H, Gersten H. *Boundary Layer Theory*. Springer: Berlin, 2000; Chap. 1.

[24] Himmelskamp H. Profile investigations on a rotating airscrew. *MAP Volkenrode Report* and Translation No. 832, 1947.

[25] Ronsten G. Static pressure measurements on a rotating and a non-rotating 2.375 m wind turbine blade. Comparison with 2D calculations. *Journal of Wind Engineering and* Industrial Aerodynamics 1992; **39**: 105-118.

[26] Dwyer HA, McCroskey WJ. Crossflow and unsteady boundary-layer effects on rotating blades. *AIAA Journal* 1971; **8**: 1498-1505.

[27] Milborrow DJ. Changes in aerofoil characteristics due to radial flow on rotating blades. *Proceedings of the 7th BWEA conference*, Oxford, 1985.

[28] McCroskey WJ. Measurements of Boundary Layer Transition, Separation and Streamline Direction on Rotating Blades. *NASA TN D-6321*, 1971.

[29] Sørensen NN, Michelsen JA, Schreck S. Navier-Stokes Predictions of the NREL Phase VI Rotor in the NASA Ames 80 ft x 120 ft Wind Tunnel. *Wind Energy* 2002; **5**: 151-169. DOI: 10.1002/we.64

[30] Lindenburg C. Modelling of rotational augmentation based on engineering considerations and measurements. *2004 European Wind Energy Conference Proceedings*, London, UK, 2004.

[31] Lindenburg C. Investigation into Rotor Blade Aerodynamics, *ECN-C--03-025*, Petten, Netherlands, 2003.

[32] Harris FD. Preliminary study of radial flow effects on rotor blades. Journal of the American Helicopter Society 1966; **11**: 1-21.

[33] Glauert H, 1963, Airplane Propellers. Aerodynamic Theory. Dover Publications: New York, 1963

[34] Sørensen JN, Myken A. Unsteady actuator disc model for horizontal axis wind turbines. *Journal of Wind Engineering and Industrial Aerodynamics* 1992; **39**: 139-149.

[35] Sørensen JN, Carsten WK, A model for unsteady aerodynamics. *Journal of Wind Engineering and Industrial Aerodynamics* 1995; **58**: 259-275.

[36] Masson C, Smaïli A, Leclerc C. Aerodynamic analysis of HAWTs operating in unsteady conditions. *Wind Energy* 2001; **4**: 1–22. DOI: 10.1002/we.43.

[37] Mikkelsen R, Actuator disc methods applied to wind turbines. *PhD Thesis*, Technical University of Denmark, Lyngby, Denmark, 2003.

[38] Sørensen JN, Shen WZ. Numerical Modeling of Wind Turbine Wakes. *Journal of Fluids Engineering* 2002; **124**: 393-399.

[39] Johansen J, Sørensen NN. Aerofoil Characteristics from 3D CFD Rotor Computations. *Wind Energy* 2004; **7**: 283-294. DOI: 10.1002/we.127.

[40] Narramore JC, Vermeland R. Navier-Stokes Calculations of Inboard Stall Delay Due to Rotation. *Journal of Aircraft* 1992; **29**: 73-78.

[41] Schmitz S, Chattot JJ. A Parallelized Coupled Navier-Stokes/Vortex-Panel Solver. *Journal of Solar Energy Engineering* 2005; **127**: 475-487.

[42] Benjanirat S, Sankar LN. Recent Improvements to a Combined Navier-Stokes Full Potential Methodology for Modeling Horizontal Axis Wind Turbines. *AIAA*-2004-0830, 23rd ASME Wind Energy Symposium, Reno NV.

[43] Lewis RI. *Vortex element methods for fluid dynamic analysis of engineering systems*. Cambridge University Press: Cambridge, UK, 1991; xix.

[44] Bertin JJ, Smith ML. *Aerodynamics for Engineers*. Prentice-Hall Inc.: Upper Saddle River, USA, 1998; 291-311.

[45] Simoes FJ, Graham JMR. A free vortex model of the wake of a horizontal axis wind turbine, *Proceedings of the 7th BWEA conference*, Norwich, UK, 1990; 161-165.

[46] Simoes FJ, and Graham JMR, Prediction of loading on a horizontal axis wind turbine using a free vortex wake model, *Proceedings of the 13th BWEA Conference*, Swansea, UK, 1991; 247-263.

[47] Simoes FJ, Graham JMR. Application of a free vortex wake model to a horizontal axis wind turbine. *Journal of Wind Engineering and Industrial Aerodynamics* 1992; **39**: 129-138.

[48] Rosen A, Lavie I, and Seginer A. A General Free-Wake Efficient Analysis of Horizontal-Axis Wind Turbines. *European Wind Energy Conference*, Madrid, Spain, 1990: 264-268.

[49] Bareiss R, Wagner S, Load Calculations on Rotor Blades of a Wind Turbine. *5th IEA Symposium*, Stuttgart, Germany, 1991; 1-10.

[50] Bareiss R, Wagner S, The Free Wake/Hybrid Wake Code RVOLM – A Tool for Aerodynamic Analysis of Wind Turbines, *Proceedings of the European Community Wind Energy Conference*, Lübeck-Travemünde, Germany, 1993; 424-427.

[51] Pesmajoglou SD, Graham JMR. Prediction of aerodynamic forces on horizontal axis wind turbines in free yaw and turbulence. *Journal of Wind Engineering and Industrial Aerodynamics* 2000; **86**: 1-14.

[52] Zervos A, Huberson S, Hemon A, Three-dimensional free wake calculation of wind turbine wakes. *Journal of Wind Engineering and Industrial Aerodynamics* 1988; **27**: 65-76.

[53] Voutsinas SG, Belessis M, Huberson S. Dynamic Inflow Effects and Vortex Particles Methods. *Proceedings of the European Community Wind Energy Conference*. Lübeck-Travemünde, Germany, 1993; 428-431.

[54] Leishman JG. *Principles of Helicopter Aerodynamics*. Cambridge University Press: New York, 2006; 589.

[55] Vermeer LJ, Sørensen JN, Crespo A. Wind Turbine Wake Aerodynamics. *Progress in Aerospace Sciences* 2003; **39**: 467–510.

[56] Leishman JG, Bhagwat MJ, Bagai A. Free-Vortex Filament Methods for the Analysis of Helicopter Rotor Wakes. *Journal of Aircraft* 2002; **39**: 759-775.

[57] Bhagwat M, Leishman JG. Stability, consistency and convergence of time marching free-vortex rotor wake algorithms. *Journal of the American Helicopter Society* 2001; **46**: 59-71.

[58] Clark DR, Leiper AC. The free wake analysis—a method for prediction of helicopter rotor hovering performance. *Journal of the American Helicopter Society* 1970; **15** : 3-11.

[59] Bhagwat MJ, Leishman JG. Time-Accurate Free-Vortex Wake Model for Dynamic Rotor Response. *Proceedings of the American Helicopter Society Specialist Meeting*, Atlanta, GA, 2000.

[60] Bagai A, Leishman GJ. Rotor Free-Wake Modeling Using a Pseudoimplicit Relaxation Algorithm. *Journal of Aircraft* 1995; **6**: 1276-1285.

[61] Bhagwat MJ, Leishman JG, On the Aerodynamic Stability of Helicopter Rotor Wakes. *Proceedings of the 56th Annual AHS Forum*, Virginia Beach, VA, 2000.

[62] Bhagwat MJ, Leishman JG. Stability analysis of helicopter rotor wakes in axial flight. *J. Am. Helicopter Assoc*. 2000; **45**: 165–178.

[63] Leishman JG, Bagai A. Challenges in Understanding the Vortex Dynamics of Helicopter Rotor Wakes. *AIAA Journal* 1998; **36**: 1130-1140.

[64] Gupta S, Leishman JG. Stability of Methods in the Free-Vortex Wake Analysis of Wind Turbines. AIAA-2004-0827.

[65] Gohard JC. *Free Wake Analysis of Wind Turbine Aerodynamics*, ASRL TR-184-14, Aero. And Struc. Research Lab., Dept. of Aeronautics and Astronautics, MIT, 1978.

[66] Afjeh AA, Keith Jr TG. A Simplified Free Wake Method for Horizontal-Axis Wind Turbine Performance Prediction. *ASME Trans. J. Fluids Eng*. 1986; **108**: 400-406.

[67] Miller RH, The Aerodynamics and Dynamic Analysis of Horizontal Axis Wind Turbines. *Journal of Wind Engineering and Industrial Aerodynamics* 1983; **15**: 329-340.

[68] Miller RH. Application of fast free wake analysis techniques to rotors. *Vertica* 1984; **8**: 255-261.

[69] Dumitrescu H, Cardos V. Predictions of Unsteady Hawt Aerodynamics by Lifting Line Theory. *Mathematical and Computer Modelling* 2001; **33**: 469-481.

[70] Kotb MA, Abdel Haq MM. A Rigid Wake Model for a Horizontal Axis Wind Turbine. *Wind Engineering* 1992; **16**: 95-107.

[71] Robison DJ, Coton FN, Galbraith RAMcD, Vezza M. Application of a prescribed wake aerodynamic prediction scheme to horizontal axis wind turbine in axial flow. *Wind Engineering* 1995; **19**: 41-51.

[72] Coton FN, Wang T, The prediction of horizontal axis wind turbine performance in yawed flow using an unsteady prescribed wake model, *Proc Instn Mech Engrs* 1999; **213 Part A**: 33-43.

[73] Wang T, Coton FN. Prediction of the unsteady aerodynamic characteristics of horizontal axis wind turbines including three-dimensional effects. *Proc Instn Mech Engrs* 2000; **214 Part A**: 385-400.

[74] Wang T, Coton FN. Numerical Simulation of Wind Tunnel Wall Effects on Wind Turbine Flows. *Wind Energy* 2000; **3**:135–148. (DOI: 10.1002/we.35).

[75] Wang T, Coton FN. A high resolution tower shadow model for downwind wind turbines. *Journal of Wind Engineering and Industrial Aerodynamics* 2001; **89**: 873–892.

[76] Schreck S, Robinson M. Boundary Layer State and Flow Field Structure Underlying Rotational Augmentation of Blade Aerodynamic Response. *Transactions of the ASME* 2003; *125*: 448-456.

[77] Schreck S, Robinson M. Rotational Augmentation of Horizontal Axis Wind Turbine Blade Aerodynamic Response. *Wind Energy* 2002; **5**: 133–150. DOI: 10.1002/we.68.

[78] The Energy Research Center of the Netherlands. *Final Report, Model Experiments in Controlled Conditions*. The Netherlands, 2007.

[79] Leishman, JG, *Principles of Helicopter Aerodynamics*, Cambridge University Press: New York, USA, 2006; 353.

[80] Hansen MOL. *Aerodynamics of Wind Turbines*. James and James: London, UK, 2000; Chap 14.

[81] Hansen MOL. *Aerodynamics of Wind Turbines*. James and James: London, UK, 2000; Chap. 17.

[82] Madsen MH, Thomsen K, Fuglsang P, Knudsen T, Two Methods for Estimating Aeroelastic Damping of Operational Wind Turbine Modes from Experiments. *Wind Energy* 2006; **9**:179–191.

[83] Hansen MH. Aeroelastic Instability Problems for Wind Turbines. *Wind Energy* 2007; **10**: 551–577. DOI: 10.1002/we.242.

[84] Riziotis VA, Voutsinas SG, Politis ES, Chaviaropoulos PK. Aeroelastic Stability of Wind Turbines: the Problem, the Methods and the Issues. *Wind Energy* 2004; **7**:373–392 (DOI: 10.1002/we.133).

[85] Hansen MH. Improved Modal Dynamics of Wind Turbines to Avoid Stall-induced Vibrations. *Wind Energy* 2003; **6**:179–195 (DOI: 10.1002/we.79).

[86] Der Spiegel. (2007, December 5). Germany commits €3.3 Billion to Combat Climate Change. *Spiegel Online International*. Retrieved March 9, 2008, from http://www.spiegel.de/international/germany/0,1518,521603,00.html

[87] Der Spiegel. (2007, December 10). UK to Expand Offshore Wind Power. *Spiegel Online International*. Retrieved March 9, 2008, from http://www.spiegel.de/international/europe/0,1518,522425,00.html

[88] Akselsen O, Ryan I, Brekk LP, Solbert E, Høybråten D, Sponheim L. (2008, January 17). Avtale om klimameldingen. *Stortinget Norge website*. Retrieved March 9, 2008, from http://www.stortinget.no/diverse/klimaforlik.html

[89] Cape Wind™. (2008, January 20). A big Cape win. *Cape Wind: Opinions and Editorials*. Retrieved March 9, 2008, from http://www.capewind.org/

[90] NAW staff. (2007, October 3). Texas Glo Awards First Offshore Wind Bid Leases in the U.S. *North American Windpower*. Retrieved March 9, 2008, from www.northamericanwindpower.com/

[91] Kowalski J. (2008, January 17). Ontario Lays Foundation for Offshore Wind Power. *Ontario Ministry of Natural Resources website*. Retrieved March 9, 2008, from http://www.mnr.gov.on.ca/

[92] Hamilton T. (2008, January 15). Ontario to approve Great Lakes Wind Power. The Toronto Star. Retrieved March 9, 2008, from http://www.thestar.com/